Renewable and Sustainable Energy Reviews 152 (2021) 111698

Contents lists available at ScienceDirect

Renewable and Sustainable Energy Reviews

journal homepage: www.elsevier.com/locate/rser

Variation of lignocellulosic biomass structure from torrefaction: A critical review

Hwai Chyuan Ong [a], Kai Ling Yu [b,c], Wei-Hsin Chen [b,d,e,*], Ma Katreena Pillejera [b,f], Xiaotao Bi [g], Khanh-Quang Tran [h], Anelie Pétrissans [i], Mathieu Pétrissans [i]

[a] Centre for Green Technology, Faculty of Engineering and Information Technology, University of Technology Sydney, NSW, 2007, Australia
[b] Department of Aeronautics and Astronautics, National Cheng Kung University, Tainan, 701, Taiwan
[c] Institute of Biological Sciences, Faculty of Science, University of Malaya, 50603, Kuala Lumpur, Malaysia
[d] Research Center for Smart Sustainable Circular Economy, Tunghai University, Taichung, 407, Taiwan
[e] Department of Mechanical Engineering, National Chin-Yi University of Technology, Taichung, 411, Taiwan
[f] College of Engineering, University of the Philippines, Diliman, Quezon City, 1101, Metro Manila, Philippines
[g] Department of Chemical and Biological Engineering, The University of British Columbia, Vancouver, BC, Canada
[h] Department of Energy and Process Engineering, Faculty of Engineering Science and Technology, Norwegian University of Science and Technology, NO-7491, Trondheim, Norway
[i] Université de Lorraine, Inra, LERMaB, F88000, Epinal, France

ARTICLE INFO

Keywords:
Biomass and bioenergy
Lignocellulosic structure
Torrefaction
Biochar
Sustainable biofuel
Thermogravimetric analysis

ABSTRACT

In recent years, torrefaction, a kind of biomass thermal pretreatment technology, has received a great deal of attention due to its effective upgrading performance of biomass. Recent studies have also suggested that the quality of syngas and bio-oil (or biocrude) from the pyrolysis, gasification, and liquefaction of torrefied biomass can be effectively improved. Torrefaction changes the structure of the biomass, the degree of this change depends strongly on the severity of the torrefaction process. To have a better understanding of the impact that torrefaction has on the biomass structure, this study aims to provide a comprehensive and in-depth review of recent advances on this topic. Particular attention is paid to biomass structure analysis through thermogravimetric analysis, scanning electron microscopy, Fourier transform infrared analysis, Brunauer-Emmett-Teller, X-ray photoelectron spectroscopy, and nuclear magnetic resonance. From these analyses, the thermal degradation characteristics of hemicelluloses, cellulose, lignin, and other components in biomass can be recognized. In addition to the elaboration of biomass structure variation from torrefaction, future challenges and perspectives are also underlined. The insights provided in this review are conducive to the further applications of biomass torrefaction for sustainable biofuel production.

1. Introduction

Nowadays, there is a huge demand for renewable and alternative energy due to the rapid growth in the global population, industrialization, and the greater necessity of fuels for transportation. Therefore, on account of the fast population growth and economic development, there is an urgent need to increase energy sources. Currently, energy consumption highly depends on the usage of conventional fossil fuels which have caused extensive damages to the atmosphere and disastrous global climate changes, as a consequence of the increasing load of carbon dioxide (CO_2) and other greenhouse gases (GHGs) [1]. To abate these issues, the development of renewable energy has drawn significant attention. Though there is a variety of sources of energy available, biomass is currently the fourth largest primary energy source in the world and serves as a potential substitute for fossil fuels [2]. Nature has provided a wide variety of biomass sources, and global biomass production was estimated to be approximately 100 billion tons annually [3]. Biomass can not only be used for food production, but it can also be considered as a potential candidate for the production of renewable fuels, carbon sequestrations, and fertilizers [4–6]. Biomass is a highly renewable and carbonaceous resource, having the potential to produce heat, electricity, fuels, chemicals, and other bio-products [7,8]. Biomass also can reduce anthropogenic carbon dioxide emissions [9,10]. Lignocellulosic biomass can be utilized for the production of biodiesel,

* Corresponding author. Department of Aeronautics and Astronautics, National Cheng Kung University, Tainan, 701, Taiwan.
E-mail addresses: weihsinchen@gmail.com, chenwh@mail.ncku.edu.tw (W.-H. Chen).

https://doi.org/10.1016/j.rser.2021.111698
Received 26 March 2021; Received in revised form 3 September 2021; Accepted 14 September 2021
Available online 27 September 2021

bioethanol, and biogas through bioconversion processes. However, it is difficult to directly ferment lignocellulosic biomass to produce bio-material, and hence a pretreatment process is needed before further utilization [11].

At present, thermochemical conversion processes, including torrefaction, pyrolysis, gasification, combustion, and liquefaction, have received much attention from many researchers and industries [12,13]. The change in the operating conditions of these methods, excluding combustion, depends on oxygen supply and reaction temperature where solid, liquid, and gas biofuels are produced. In general, biomass pyrolysis is conducted at temperatures between 400 °C and 800 °C, and can be categorized into fast pyrolysis, slow pyrolysis, catalytic pyrolysis, and microwave pyrolysis [14–17]. Liquefaction is a thermal process at a temperature range of 200–400 °C at higher pressures (10–25 MPa) to convert biomass into bio-crude oil [18]. The gasification process takes place at relatively high temperatures under low oxygen conditions for the transformation of biomass [19].

In thermochemical techniques, the direct use of raw biomass faces many issues such as high moisture content, lower heating value, volatility, and low energy density when compared to fossil fuels [20]. In addition, it also causes other problems like smoke emissions during combustion, hygroscopic nature, uneven/heterogeneous composition, and transportation difficulties [21]. Hence, to overcome these issues, biomass needs to be pretreated to enhance the quality of producing energy conversion materials. Torrefaction is a promising pretreatment technology to upgrade biomass for solid fuel production and to offset greenhouse gas emissions. In this method, biomass is exposed to an inert atmosphere at low temperatures and is converted into a charcoal-like carbonaceous material holding excellent properties [22,23].

In general, raw biomass, which is targeted for use as fuel, has some drawbacks such as low calorific value, high moisture content, low energy density, non-homogeneous, poor grindability, significant inorganic substances, low combustion efficiency, etc., thereby reducing its viability as a solid biofuel feedstock [24]. Torrefaction not only improves the fuel characteristics of biomass, such as carbon content and calorific value but also enhances hydrophobicity and grindability. It also lowers biodegradation and delivers a higher storability with low moisture content [15,25]. To enhance the physical and chemical characteristics of lignocellulosic biomass as a viable substitute for coal, torrefaction pretreatment has been explored extensively [26]. Torrefaction may effectively reduce the oxygen-to-carbon ratio (C/O) in cellulose and hemicelluloses [27,28]; it may also cause polycondensation and de-methoxylation of the aromatic units of lignin [29]. As the torrefaction temperature increases, the solid yield gradually decreases, as a result of the release of moisture and volatiles [30,31], whereas gaseous and liquid products gradually increase. In the low-temperature range, the reduction in the solid yield is relatively low [32,33]. Although torrefied products hold many advantages, some advanced techniques are still needed in production for commercialization to be consolidated within the global matrix of energy production.

To date, there is a limited literature review focused on the impact of torrefaction on lignocellulosic biomass *via* structure analysis. Therefore, this study aims to investigate the current pretreatment options on lignocellulosic biomass by identifying the main strengths and weaknesses of each one of these options. This review also provides significant comparisons on the impact of torrefaction on lignocellulosic structure based on several characterization methods, keeping into consideration recent developments on the torrefaction process. Several structural analyses such as thermogravimetric analysis (TGA), scanning electron microscope (SEM), Fourier transform infrared (FTIR), X-ray diffraction (XRD), Brunauer-Emmett-Teller (BET), X-ray photoelectron spectroscopy (XPS), and nuclear magnetic resonance (NMR) are discussed. These analyses characterize and determine the structures and properties of lignocellulosic biomass undergoing torrefaction. Fig. 1 shows a summary of the structural analysis that can be carried out to characterize the lignocellulosic biomass.

2. Lignocellulosic biomass structure

Lignocellulosic biomass is known as a sustainable and one of the most abundant energy sources, which is available all over the world. Lignocellulosic biomass is non-edible and is mainly present in forest and agricultural biomass [34,35]. Furthermore, most of the lignocellulosic biomass is simply disposed of as waste material. In developing countries, communities from rural areas mainly rely on traditional energy sources such as crop residues, firewood. The traditional way to obtain energy is not only expensive and inefficient, but the process is also time-consuming and causes harmful pollution to the environment. The lignocellulosic biomass will be able to provide approximately 38% of the worldwide direct fuel supply and 17% of the world's electricity by 2050 [36,37].

Generally, all plant materials are composed of three major components, namely, cellulose, hemicelluloses, and lignin [38]. These three major components are unevenly distributed in the cell wall and provide a skeleton structure for the plants [39]. The connection between cellulose and hemicelluloses or lignin occurs mainly through hydrogen bonds, while the connection between hemicelluloses and lignin occurs by both hydrogen and covalent bonds [40,41]. Concerning the structure, cellulose is a glucan polymer of D-glucopyranose units that are linked together by β-(1–4)-glycosidic bonds [42]. Meanwhile, hemicelluloses

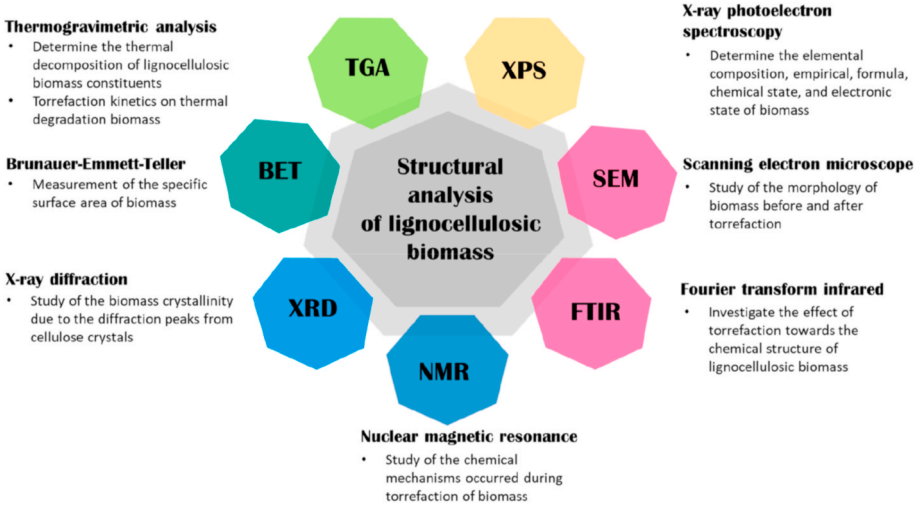

Fig. 1. Summary of the structural analysis of lignocellulosic biomass.

consist of polysaccharide polymers with a lower degree of polymerization compared to cellulose. Hemicellulose contains mainly sugars such as D-xylopyranose, D-glucopyranose, D-galactopyranose, L-arabinofuranose, D-mannopyranose, D-glucopyranosyluronic acid and D-galactopyranosyluronic acid, etc. [43,44]. Furthermore, lignin has its own characteristics such as being three-dimensional, amorphous, and a highly branched-phenolic polymer [45]. Lignin is formed through an irregular biosynthesis process constructed from three basic phenylpropanoid monomers, *p*-hydroxyphenyl (H), guaiacyl (G), and syringyl (S) units [46]. Biomass is composed of about 20–30% of hemicelluloses, 10–25% of lignin, and 40–50% of cellulose [47,48]. However, the study has found that there is no synergistic effect from the co-torrefactions of the blend of hemicelluloses, cellulose, and lignin. The weight losses of the three blend components were similar to those individual components [49]. Based on this result, it may be inferred that the impact of co-torrefaction of the three components on the lignocellulosic structure is slight. Apart from these cell wall components, a small fraction of extractives and inorganic ash also exist as non-structural components in biomass, and they are not constituted with the cell layers. Usually, woody biomass comprises 90% of cellulose, hemicelluloses, and lignin, while agricultural biomass contains more extractives and ash.

Currently, lignocellulosic biomass can be utilized through direct combustion to produce heat. This method generates heat and must be exploited immediately for heating or power generation. However, this approach has a significant problem of low energy efficiency, it also may lead to global warming from the harmful emissions of large amounts of carbon dioxide to the environment. Thus, the researchers showed considerable attention to the conversion of biomass to bioenergy through the biochemical or thermochemical process [29].

In the thermochemical process, heat and catalysts are used to convert biomass into bioenergy, whereas enzymes and microorganisms are widely used in the biochemical process [50]. In comparison to

Table 1
Lignocellulosic biomass under various pyrolysis processes and their main products.

Lignocellulosic biomass	Pyrolysis process	Process conditions	Main products	Ref.
Camellia oleifera shell	Microwave-assisted pyrolysis	500 °C, 20 min	• Bio-oil: 37.30–40.27 wt% • HHV: 21.37–23.77 MJ/kg • With the distribution of solid and gas products	[198]
Corncob	Fast pyrolysis for saccharification	500 °C, 20 s (10, 20, 40, 80 °C min^{-1})	• Solid yield: 10.1–25.8% • Multifarious derivatives of anhydrosugar, levoglucosan as the major product	[199]
Quercus rubra (red oak) wood chips	Autothermal/partial oxidative pyrolysis	500 °C, 0.7 s, air	• Marginally change the chemical composition of phenolic compounds in bio-oil compared to conventional fast pyrolysis	[200]
Bamboo	Fast pyrolysis	900 °C, 2 h, 45 °C min^{-1}, N_2 gas	• Solid yield: 48.8–50.9% (lignin); 21.1–24.3% (hemicellulose); 8.3–11.4% (cellulose) • Major volatile products: acetone, acetic acid (lignocellulose); aromatic compounds (lignin)	[201]
Canadian pinewood	Catalytic pyrolysis	500 °C, 50 °C min^{-1} amorphous silica-alumina catalyst	• Solid HHV: 14.97 MJ/kg (Cellulose); 15.31 (Hemicellulose) • Catalytic derived bio-oil: 25.22 MJ/kg (Lignin); 34.20 MJ/kg (Cellulose); 34.40 MJ/kg (Hemicellulose); 39.70 MJ/kg (Lignin) • Majority aliphatic hydrocarbons from lignin	[202]
Bamboo *(Bambusa balcooa)*	Pyrolysis (with condensable volatiles quantification by thermogravimetric analysis)	30–600 °C, 10 °C min^{-1}, inert atmosphere	• Total volatile compounds yield: 18.68 wt% with 16.27 wt % (carbohydrates-derived); 1.12 (lignin-derived) • Solid yield: 28.58 wt%	[203]
Pine *(Pinus radiata)*			• Total volatile compounds yield: 18.10 wt% with 16.01 wt % (carbohydrates-derived); 1.52 (lignin-derived) • Solid yield: 22.34 wt%	
Corn cob			• Total volatile compounds yield: 15.02 wt% with 13.65 wt % (carbohydrates-derived); 0.95 (lignin-derived) • Solid yield: 23.21 wt%	
Corn stover			• Total volatile compounds yield: 17.22 wt% with 15.95 wt % (carbohydrates-derived); 0.69 (lignin-derived) • Solid yield: 27.68 wt%	
Lignocellulose fermentation residue	Pyrolysis (fixed-bed microreactor)	25–800 °C, 10 °C min^{-1}, N_2 gas	• Gas yield: 15–31% • Solid yield: 50–60% • Liquid yield: maximum 25% • The liquid phase was mainly composed of phenols	[204]
Beechwood	Catalytic fast pyrolysis	500 °C, 30 min, N_2 gas, with HZSM-5 and Al-MCM-41 catalysts	• Oil yield: 9.07–23.37% • Water yield: 31.92–43.09% • Gas yield: 18.11–22.34% • Solid yield: 24.57–26.60%	[205]
	Thermal pyrolysis		• Oil yield: 28.43% • Water yield: 28.87% • Gas yield: 11.93% • Solid yield: 30.77%	
Canadian pinewood	Catalytic pyrolysis	450 °C, 1 bar, Ar gas, amorphous silica-alumina catalyst	• Organics yield: 23.1–42.4 wt% • Water yield: 19.1–27.1 wt% • Gas yield: 10.5–17.1 wt% • Solid yield: 17.6–19.3 wt%	[206]
Willow wood	Slow pyrolysis	200–350 °C, 5 °C min^{-1}, 10 min, N_2 gas	• Biochar yield: 39.8–98.1 wt%	[207]
	Microwave pyrolysis	170 °C	• Biochar yield: 27.3 wt%	
Mixed straw pellets	Slow pyrolysis	200–350 °C, 5 °C min^{-1}, 10 min, N_2 gas	• Biochar yield: 46.4–93.9 wt%	
	Microwave pyrolysis	200 °C	• Biochar yield: 33.7 wt%	

biochemical processes, the thermochemical process is a better option in that it has a shorter process time. Besides, the biochemical conversion is an expensive and difficult process that requires hydrolytic pretreatment (enzymatic, acid/base, or hydrothermal) to separate cellulose, hemicelluloses, and lignin components in the lignocellulosic biomass [51]. In this process, the cellulose fraction can be fermented into alcohol, however, lignin showed a negative result [52]. Therefore, the degradation of lignin is possible only through combustion or thermochemical conversion technologies. Moreover, there are no other feedstocks that can be utilized with a significantly higher conversion yield of the product in the thermochemical process [53]. Torrefied biomass has greater potential with improved thermal characteristics, which provides a more stable condition to hold higher energy value and helps in the reduction of greenhouse gases (GHGs) emissions to the atmosphere. Table 1 lists recent studies on lignocellulosic biomass under various pyrolysis processes and their main products.

3. Torrefaction

Lately, biomass pretreatment using the torrefaction process has received significant attention from researchers on promising applications. Torrefaction is defined as a thermal process to convert biomass into bio-coal, and this emerging technology shows satisfactory results according to several works of literature on different kinds of biomass sources [54]. Torrefaction is a mild pyrolysis process that occurs at temperatures between 200 and 300 °C [55–57] under an oxygen-deficient environment for appropriate durations (0.5–2 h). At the end of the torrefaction process, the components of hemicelluloses, lignin, and cellulose are decomposed and a high amount of volatile compounds is emitted [58]. During torrefaction, carboxyl and conjugated ketone are generated by the processes of dissociation of O-acetyls and dehydration of hydroxyls in hemicelluloses [59], anhydrosugar in the torrefaction of cellulose [60], and phenols in the torrefaction of lignin [61]. The solid yield from hemicellulose torrefaction is commonly the lowest compared to cellulose and lignin [60,62]. The gaseous products in torrefaction from major components (cellulose, hemicelluloses, and lignin) are mainly CO_2 and CO, followed by a small amount of CH_4 and H_2 [61,63]. Meanwhile, in the liquid products, the dominant compounds are dehydrosugars from cellulose, furfural and acetic acid from hemicelluloses, and phenols from lignin [29,61]. The three main products of torrefaction are in the forms of liquid, solid, and non-condensable gases. A schematic diagram of torrefaction process is shown in Fig. 2 and the phases in the torrefaction process is shown in Fig. 3. However, the aim of this process is to obtain solid torrefied biomass, a type of biochar. Table 2 shows recent studies on the torrefaction technology of lignocellulosic biomass and their product properties.

The torrefied biomass (biochar or black carbon) is a stable and carbon-rich solid bio-product [64,65]. In this process, biomass is dried and a large amount of CO (~20%) and CO_2 (~80%) with some volatile compounds are released [66]. Consequently, the biomass weight can be reduced by 30%–70% and the torrefied biomass can stow 90% of the energy after torrefaction [67]. The change of biomass structure is closely related to the physicochemical properties of biomass, such as hydrophobicity, mechanical strength, element content, and so on. Some of the notable findings in the changes with the physicochemical properties due to torrefaction are listed in Table 3. Torrefied biomass contains a higher calorific value due to the higher *C*–C and *C*–H bonds, and a higher

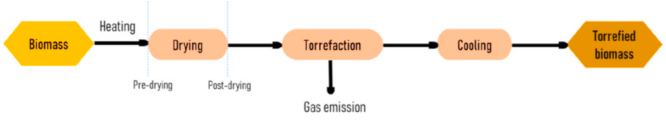

Fig. 2. Schematic diagram of torrefaction process.

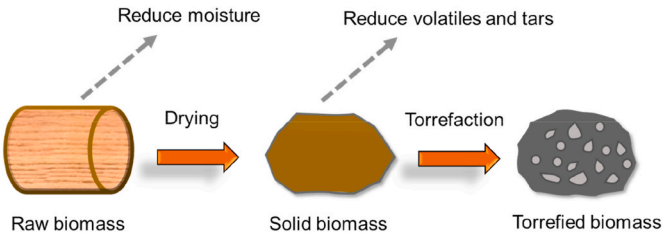

Fig. 3. Phases in the torrefaction process.

amount of energy is released from *C*–C and *C*–H bonds compared to O–H and *C*–O bonds present in untorrefied biomass [68]. The literature survey shows that torrefied biomass has lower atomic O/C and H/C ratios because of higher-temperature pretreatment, and this makes the torrefied product similar to coal [69,70]. This technique also enhances the grindability and durability of biomass, and shows better performance in combustion, gasification, and co-firing purposes [71,72]. Also, the biomass attained after torrefaction contains less amount of ash content from wet torrefaction, and it is more environmental-friendly than other fossil fuels from the perspective of net greenhouse gas emissions [73]. Furthermore, torrefaction process parameters such as temperature, residence time, heating rate, biomass moisture content, particle size possess a direct impact on the final torrefied biomass properties [74]. Torrefaction is generally performed at low temperatures with a short residence time using a low heating rate for a higher final solid yield [75]. The product yield is highly influenced by the torrefaction temperature where the solid yield decreases with increasing temperature, while liquid and gas product yields increase with the increase of temperature [74]. Apart from temperature, the residence time is also a significant factor for the properties of torrefied biomass. A short torrefaction residence time (15–60 min) is adequate for a complete torrefaction process on biomass, and prolonging the residence time does not show a significant effect on biomass transformation [15,76]. The heating rate is also one of the influencing factors in torrefaction where a lower heating rate (<50 °C min^{-1}) is favorable for the higher yield of solid torrefied biomass [77]. The moisture content of biomass generally possesses an impact on the energy conversion process during torrefaction, where the moisture content of the raw biomass shall be kept at minimal for dry torrefaction [74]. Biomass particle size has a less significant influence on the torrefaction process compared to temperature and residence time. However, the particle size should be taken into account to allow uniform heating of biomass in terms of mass transfer throughout torrefaction for better solid and energy yields [78]. It can be concluded that torrefaction severity influences the torrefied biomass properties where further optimization of the parameters will be needed based on the desirable application.

Torrefaction is also able to alter the biomass components distribution where cellulose and hemicelluloses degradation usually occurs at temperatures between 200 and 400 °C [79,80], and lignin degrades slowly at a higher temperature range of 200–900 °C. Torrefaction also helps to reduce the hemicellulose content from 22% to 4.6% at 300 °C, while cellulose degraded slowly and the lignin content increased [81]. Chen and Kuo [82] studied the effects of dry torrefaction on bamboo, coconut shell, willow, and wood at a temperature of 240 °C. They found that hemicelluloses degraded completely at this temperature; nonetheless, no degradation was observed in cellulose or lignin. Similarly, another study [83] also observed that the degradation of hemicelluloses started to occur in dry torrefaction at a temperature of 180 °C. Torrefaction also plays a role in changing the chemical structure of cell and cell wall components. The changes in biomass physical structure during torrefaction bring up new opportunities for biomass applications. Torrefaction removes water from biomass, causes hemicellulose depolymerization, and results in a stable physical condition. Industrial carbonization, polymer compounding, and other carbon-related

Table 2
Torrefaction technology of lignocellulosic biomass and their product properties.

Biomass	Torrefaction technology	Torrefaction condition	Torrefied product properties	Ref.
Loblolly pine	Wet torrefaction	200–260 °C, 200–700 psi, 15–30 min, hot compressed water, N_2 gas	Solid yield: 57.0–88.7% HHV: 5043.3–6342.5 cal/g Energy yield: 77.5–95.8%	[208]
	Dry torrefaction	250–300 °C, 80 min, N_2 gas	Solid yield: 60.5–83.8% HHV: 5005.4–5627.4 cal/g Energy yield: 73.2–89.7%	
Sawdust	Non-oxidative torrefaction	240–300 °C, 50 and 120 min	Solid yield: 32.6–65.1% HHV: 19.56–25.95 MJ/kg Energy yield: 73.3–99.6%	[209]
	Oxidative torrefaction	240–300 °C, 50 and 120 min, O_2 gas	Solid yield: 41.3–60.1% HHV: 19.30–23.50 MJ/kg Energy yield: 65.7–94.5%	
Poplar wood	Dry torrefaction	200–320 °C, 15–120 min, 25 °C min^{-1}, N_2 gas or semi-closed system	Solid yield: 20.1–66.5% HHV: 18.36–27.81 MJ/kg	[210]
Willow	TGA-FTIR torrefaction	503–563 K, 30 min, 20 K min^{-1}, N_2 gas	Solid yield: 72.0–95.1% HHV: 20.2–21.9 MJ/kg Energy yield: 79.2–96.5%	[211]
Reed canary grass			Solid yield: 61.5–92.6% HHV: 20.0–21.8 MJ/kg Energy yield: 69.0–93.5%	
Wheat straw			Solid yield: 55.1–91.0% HHV: 19.4–22.6 MJ/kg Energy yield: 65.8–93.5%	
Rice husk	Oxidative torrefaction	220–300 °C, 30 min, 0–15 vol% O_2	Solid yield: 55–85% Energy yield: 64–89%	[212]
	Non-oxidative torrefaction	220–300 °C, 30 min, N_2	Solid yield: 92.71% HHV: ≤18.91 MJ/kg Energy yield: 80.56%	
Azolla filiculoides (mosquito fern)	Dry torrefaction Hydrothermal carbonization	260–300 °C, 15 min, 10 °C min^{-1}, Ar gas 260–300 °C, 15 min, 8–10 °C min^{-1}, 60–83 bar, N_2 gas	Solid yield: 67.1–83.8% Solid yield: 33.8–66.8%	[213]
Sugarcane bagasse	Dry torrefaction	200–275 °C, 15–60 min, 20 °C min^{-1}, N_2 gas	Solid yield: 54–80% HHV: ≤24.01 MJ/kg Energy yield: 69–89%	[214]
Textile sludge with agricultural and lignocellulosic biowaste	Microwave-assisted wet torrefaction/ Co-torrefaction	120–180 °C, 15 °C min^{-1},10–30 min	HHV: 17.3–20.9 MJ/kg Energy yield: 84.3%	[215]
Bamboo residue	Dry torrefaction	200–300 °C, 60 min, 10 °C min^{-1},N_2 gas	Solid yield: 49.48–86.24% HHV: 17.57–21.96%	[216]
Corncob	Dry torrefaction	210–300 °C, 30 min, 15 °C min^{-1}, N_2 gas	Solid yield: 36.05–81.28% HHV: 20.11–28.09 MJ/kg Energy yield: 54.26–87.58%	[217]
Pigeon pea stalk	Dry torrefaction	200–300 °C, 0–60 min, 5–20 °C min^{-1}, N_2 gas	HHV: 17.84–24.23 MJ/kg Energy yield: 57.49–94.65%	[218]
Plywood	Dry torrefaction	200–300 °C, 5–120 min, N_2 gas	Solid yield: 52.26–96.68 wt % Energy density ratio: Highest 1.23	[219]
Fibreboard			Solid yield: 50.18–97.02 wt % Energy density ratio: Highest 1.24	
Particleboard			Solid yield: 48.43–96.55 wt % Energy density ratio: Highest 1.17	
Commercial fir pellets	Non-oxidative torrefaction	200–250 °C, 15 min, N_2 gas	Solid yield: 52.72–90.12 wt % Liquid yield: 3.68–18.90 db HHV: 20.71–24.20 MJ/kg Energy yield: 65.06–93.65%	[220]
Olive pomace pellets			Solid yield: 56.34–79.92 wt % Liquid yield: 3.37–13.8 db HHV: 24.42–27.16 MJ/kg Energy yield: 75.22–94.50%	
Commercial fir pellets	Oxidative torrefaction	200–250 °C, 15 min, 20 °C min^{-1}, air	Solid yield: 38.23–86.61 wt % Liquid yield: 4.17–27.30 db HHV: 20.35–25.06 MJ/kg	

(*continued on next page*)

Table 2 (*continued*)

Biomass	Torrefaction technology	Torrefaction condition	Torrefied product properties	Ref.
Olive pomace pellets			Energy yield: 49.85–88.35% Solid yield: 53.04–71.41 wt % Liquid yield: 10.34–24.7 db HHV: 23.53–26.15 MJ/kg Energy yield: 68.40–82.12%	

Table 3
Changes in the physicochemical properties of biomass due to torrefaction.

Physicochemical properties	Findings	Ref.
Surface morphology	Changes in the surface morphology of biomass were closely related to the moisture in biomass and the release of volatiles. Slow vaporization of internal moisture of the biomass pellets is the major reaction at lower temperatures. As the torrefaction temperature increases, a large amount of volatile gas accumulated in a short time, creating relatively higher pressure within the pellets, thus, damaging the surface morphology.	[221]
Hydrophobicity	Torrefaction produces a hydrophobic product by destroying OH groups and causing the biomass to lose the capacity to form hydrogen bonds. Due to these chemical rearrangement reactions, non-polar unsaturated structures are formed, which preserve the biomass for a long time without biological degradation, similar to coal.	[222]
Hygroscopicity	The reduction of Equilibrium Moisture Content (EMC) could be attributed to the release of extractives which are mainly consisted of organic volatile products condensed inside the wood pores. The lower saturated moisture content in torrefied biomass could also result from tar condensation inside the pores of torrefied biomass, obstructing the passage of moist air through the solid, and then avoiding the condensation of water vapor. In addition, the apolar character of condensed tar on the solid also prevents the condensation of water vapor inside the pores.	[223]
Mechanical strength	During the torrefaction process the biomass tends to shrink; become lightweight, flaky, and fragile; and lose its mechanical strength, making it easier to grind and pulverize.	[224]
Grindability	During the torrefaction process, the biomass loses its tenacious nature, which is mainly coupled to the breakdown of the hemicellulose matrix and depolymerization of the cellulose, resulting in the decrease of fiber length. The decrease in particle length, but not in diameter per se, results in better grindability, handling characteristics, and flowability through processing and transportation systems.	[222]
Elemental composition	As the torrefaction temperature increases, the elemental carbon content of torrefied biomass increases, while hydrogen and oxygen contents decrease due to the release of volatile being rich in hydrogen and oxygen, such as water and CO_2, which results in decreased H/C and O/C ratios and makes the fuel properties shift towards coal.	[225, 226]

operations may now use torrefied biomass as a resource for the application [84]. Dry torrefaction technology has progressed significantly to the extent of commercialization and market launch. Several torrefaction plants have subsequently been developed in Europe and North America [85]. According to recent market statistics, the torrefaction technology market will be processing over 130 million tons per year by 2020 [86]. In addition, torrefaction can enhance the compatibility of biomass for co-firing in coal-fired power plants, potentially facilitating the higher co-firing percentages at lower costs [87]. The torrefied biomass possesses a more uniform product quality after torrefaction. Besides, the torrefied biomass is in ease of storage due to the decomposition behavior and hygroscopicity [88,89]. This decouples the production and consumption of large-scale torrefied biomass from the seasonal dependence of biomass availability. The enhancement of torrefied biomass properties also makes it an attractive solid fuel for energy conversion processes with an increase in grindability and promising in-situ processing characteristics [90]. The low moisture content of biomass after torrefaction also contributes to cleaner gas production and stable quality. These improvements in the torrefied biomass properties are advantageous and provide the ability to process torrefied biomass on existing coal infrastructure without the need for significant additional investment [15].

According to biomass nature, torrefaction can be divided into two types such as dry and wet processes. In a dry torrefaction process, a controlled heating condition of biomass is applied under an inert atmosphere (N_2 or CO_2) with low oxygen availability. In this technology, the product is obtained after partial degradation and without combustion [62,91]. This method also improves the microbe's resistance and water vapor absorption. Whereas, in wet torrefaction, partial degradation is applied under controlled conditions through heating in hot water or steam under high pressures [92]. Generally, the temperature required for dry torrefaction (200–300 °C) is slightly higher than the wet torrefaction method (150–260 °C). Both of the torrefaction methods show advantages and disadvantages. For example, the wet method requires more advanced equipment, and thus the investment cost is higher. In contrast, dry torrefaction is considered as a potential pretreatment technology to produce biomass that is more suitable for bioenergy applications, with a significant amount of ash content remaining after the process [93]. However, a biomass sample with a high amount of ash may cause undesirable operational problems in boilers such as fouling, slagging, corrosion, and agglomeration [94]. Other than that, dry torrefaction also possesses a disadvantage where biomass pre-drying is required prior to the dry torrefaction process [15]. In addition, wet torrefaction also possesses some limitations. For example, post-drying will be needed to obtain the dry torrefied biomass and the operation is under high pressure. Also, there might be some corrosion in the reactor by chemicals such as inorganic salts, and this will be a challenge for continuous production [15].

The conventional torrefaction technology exhibits a limited deoxygenating effect due to mild operating conditions and thus some recently improved torrefaction techniques are being proposed by other researchers, for example, pressurized torrefaction, mechanically pressurized torrefaction, torrefaction in a closed system, etc. A study on novel gas-pressurized torrefaction has been carried out and showed the production of torrefied biomass with a higher oxygen removal efficiency of 65% in biomass compared to conventional torrefaction at a relatively low temperature [25]. Gas-pressurized torrefaction improved the biomass properties for subsequent pyrolysis and a lignin-like structure. The study on upgrading of woody leucaena biomass through torrefaction under volumetric pressure was carried out [95]. There was an increase in the yield of torrefied biomass with increasing pressure, and

the pressurized torrefaction changed the structure of biomass with an enhancement for the cross-linking reaction throughout pyrolysis, resulting in higher char product yield. Torrefaction under pressure could upgrade the quality of biomass efficiently. Nonetheless, the high pressure would induce a higher energy consumption and thus a high cost for practical application. Therefore, further optimization on the pressure variation of these recent techniques is needed. Other than that, microwave torrefaction was also proposed for the pretreatment for high-moisture biomass waste where the process could enhance the latter gasification performance in the approach of clean technology [96]. In addition, the study on microwave wet torrefaction with catalytic approach also showed potential in treating lignocellulosic biomass waste with better efficiency and enhanced properties for torrefied biomass. The upgrading of the current torrefaction technology would provide better efficiency to the system, but there is no suggested reactor type for the optimized process where the selection will be correlated to the types of biomass and process conditions [97]. Further research on these technologies should be addressed to make them successful at the commercial level.

It is important to explore the different structural characteristics of biochars, and this will greatly deepen our understanding of the function manipulation of biochar production. The establishment of the relationship between biochar structures and their physicochemical properties will eventually enable the production of the biochars with specific structures, such as engineered adsorbents, which can have their own application, for instance, soil remediation.

Table 4
DTG peak on the impact of torrefaction temperature on the weight loss percentage of different lignocellulosic biomass constituents under several torrefaction severities.

Biomass constituents/Biomass	Reaction temperature (°C)	Weight loss (%)	Ref.
Hemicellulose	200	0.8	[100]
	225	2.3	
	250	19.5	
	275	52.6	
	300	16.8	
Cellulose	200	0.5	
	225	1.2	
	250	3.0	
Lignin	300	7.4	
Xylan	250	14.6	
	275	8.0	
	300	3.5	
Hemicellulose	230	2.74	[49]
	260	37.98	
	290	58.33	
Cellulose	230	1.05	
	260	4.43	
	290	44.82	
Lignin	230	1.45	
	260	3.12	
	290	6.97	
Xylan	230	14.16	
	260	17.10	
	290	3.94	
Dextran	230	4.92	
	260	26.39	
	290	14.66	
Douglas fir sawdust	250	12	[227]
	275	26	
	300	48	
Willow, reed canary grass, wheat straw	290	27–38	[103]

4. Structure analysis

4.1. Thermogravimetric analysis (TGA)

Thermogravimetric analysis is typically carried out using a thermogravimetric analyzer (TG) to investigate the thermal decomposition behavior of a substance with measurement of the amount and percentage of change in weight as a function of temperature. Biomass is loaded into a crucible and placed in a TG before heating up at a selected heating rate and a temperature range under the inert condition to measure the biomass weight. TGA and derivative thermogravimetric (DTG) analysis can be obtained from the recorded distribution of the biomass weight loss. The biomass weight and its change rate due to dehydration, decomposition, and oxidation are derived from the TGA graph, and the biomass weight loss to temperature is derived from the DTG graph [98]. The remaining char residue of biomass after TGA analysis shows the distinct difference in the weight loss curve, the weight loss percentage increases with the torrefaction temperature from raw sample to torrefied biomass samples [99]. The thermal decomposition and torrefaction kinetics of lignocellulosic biomass can be further examined through TGA.

4.1.1. Thermal decomposition of lignocellulosic biomass

Thermogravimetric analysis can be carried out to study the effect of the torrefaction process on thermal decomposition of few basic lignocellulosic biomass constituents such as hemicelluloses, cellulose, lignin, and xylan which is a subgroup from hemicelluloses [100]. When torrefying biomass, the particle size is an important parameter due to varying conditions experienced by reaction intermediates. The torrefaction rate will be influenced by the particle size, especially at high temperatures. The results have shown that the energy and mass yields increased with the length-to-diameter ratio of the biomass particles [101]. Moreover, different severity levels of torrefaction give different impacts on the thermal degradation of each of the lignocellulosic biomass constituents as well. The torrefaction process alters the physicochemical properties of biomass, and hence the moisture content in biomass is reduced. In general, hemicelluloses in biomass will be degraded by torrefaction due to high temperatures, whereas the degradation extents of cellulose and lignin will occur based on the applied torrefaction temperatures [82,102]. The literature studies of DTG highlighting the impact of torrefaction temperature on the weight loss percentage of different lignocellulosic biomass constituents under several torrefaction severities are shown in Table 4.

It is notable that, even at a low torrefaction temperature of 230 °C, hemicelluloses are significantly altered by the torrefaction procedures. According to the study of Bridgeman et al. [103], they showed that the decomposition of hemicelluloses using xylan constituents occurred at temperatures above 200 °C, where full devolatilization took place at 350 °C to form major products such as H_2O, CO_2, CO, and char along with small amounts of organic products [104]. However, cellulose is only affected when severe torrefaction (290–300 °C) is employed. Cellulose has a slower decomposition reaction at temperatures below 250 °C compared to hemicelluloses. However, the thermal decomposition rate increases when the reaction temperature is increased up to above 300 °C. At the temperature range of 250–300 °C, the devolatilization of polysaccharides will occur up to 20–30% [105]. The mass loss that occurs at these temperatures is due to the depolymerization reactions that cause a reduction in the length of polysaccharide polymers from 1000 to 200 monomer units [106]. Other than that, there is just a small influence on the lignin component when either severity level of torrefaction is applied [100]. Overall, the thermal decompositions of hemicelluloses, cellulose, and lignin occur at the temperature ranges of 220–315 °C, 315–400 °C, and 160–900 °C, respectively [82,107–109].

4.1.2. Kinetics

Thermogravimetric analysis (TGA) is used as a common thermoanalytical method to study the thermal degradation and thermal behavior

Table 5
Literature studies on the kinetic parameters of lignocellulosic biomass and/or its constituents from different models.

Biomass components	Order of reaction, n (−)	Activation energy, *Ea* (kJ mol^{-1})	Pre-exponential factor, *A* (min^{-1})	Ref.
Hemicellulose	3	187.06	4.13×10^{16}	[100]
Cellulose	1	124.42	2.86×10^{9}	
Lignin	1	37.58	6.625	
Xylan	9	67.83	7.28×10^{25}	
Alstonia congensis (Ahun)	2.28	143.38	1.90×10^{10}	[228]
Ceiba pentandra (Araba)	2.15	134.45	1.83×10^{13}	[228]
Corn stalk	–	184.10	–	[30]
Corn stalk	–	193.00	–	[30]
Corn stalk	–	48.47	6.56	[229]
Olive tree pruning	–	46.23	6.04	[229]
Vine pruning	–	60.89	6.37	[229]
Olive pomace	–	167.94–994.09	–	[230]
Olive pomace	–	162.59–1069.74	–	[230]
(Raw spruce woods) Hemicellulose	1	103.80	3.70×10^{7}	[231]
Cellulose	1	221.58	2.43×10^{17}	
Lignin	1	66.17	1.33×10^{3}	
Char	1.01	178.48	5.92×10^{10}	
(Wet torrefied spruce woods at 210 °C) Hemicellulose	1	47.01	2.88×10^{2}	[231]
Cellulose	1	250.49	9.17×10^{19}	
Lignin	1	83.68	3.63×10^{4}	
Char	1.02	127.32	4.27×10^{6}	
(Wet torrefied spruce woods at 222 °C) Hemicellulose	1	41.48	8.08×10^{1}	[231]
Cellulose	1	247.92	5.39×10^{19}	
Lignin	1	81.30	2.26×10^{4}	
Char	1.01	134.06	1.43×10^{7}	
(Dry torrefied spruce woods at 275 °C) Hemicellulose	1	–	–	[231]
Cellulose	1	221.25	4.26×10^{17}	
Lignin	1	72.78	3.18×10^{3}	
Char	1.07	239.28	1.44×10^{15}	
Cellulose	–	119.21	6.9×10^{9}	[232]
Xylan	–	116.84	5.4×10^{11}	
Lignin	–	43.29	1.4×10^{3}	
Cellulose	–	227.02	5.6×10^{16}	[233]
Xylan	–	69.39	2.1×10^{3}	
Lignin	–	7.8	4.9×10^{-5}	

of lignocellulosic biomass [110,111]. Generally, with torrefaction as an isothermal pretreatment process, the torrefaction kinetics based on TGA data can be used to provide the prediction on isothermal degradation of biomass [100,112]. Thermal decompositions of lignocellulosic constituents, namely, hemicelluloses, cellulose, lignin, and xylan can be studied and predicted using isothermal kinetics. Torrefaction kinetics shows its importance in determining the thermal degradation and conversion of substances and product formation, other than contribution in prediction of experimental design, process rate, selection of operational parameter, and practical operation [113].

According to the study of Bach and Chen [112], the torrefaction kinetics was expressed in Arrhenius law which included the reaction order, activation energy, and frequency factor. The reaction rate under an isothermal condition with changes over time was denoted in equation (1):

$$\frac{d\alpha}{dt} = k(T)\cdot f(\alpha) = Aexp\left(\frac{-E_a}{RT}\right)\cdot f(\alpha) \quad (1)$$

where α is conversion degree, t conversion time, A pre-exponential factor, E_a activation energy for the reaction, R universal gas constant, and T absolute temperature. The mass fraction of decomposed solid or released volatiles was denoted as the conversion degree α which is defined in equation (2):

$$\alpha = \frac{m_0 - m}{m_0 - m_f} = \frac{v}{v_f} \quad (2)$$

where m_0 is the initial mass of solid, m_f the final mass of solid, m the mass of solid at a given time, v_f the total released mass of volatiles, and v the mass of released volatiles at a given time.

For a non-isothermal expression, the reaction rate in Eq. (1) is transposed to describe the conversion rate as a function of temperature at a constant heating rate (β), as shown in equation (3):

$$\frac{d\alpha}{dT} = \frac{dt}{dT}\frac{d\alpha}{dt} = \frac{1}{\beta}\frac{d\alpha}{dt} \quad (3)$$

Hence, the non-isothermal rate is expressed from the substitution of Eq. (1) into Eq. (3) as shown in equation (4):

$$\frac{d\alpha}{dT} = \frac{k(T)}{\beta}\cdot f(\alpha) = \frac{A}{\beta}\exp\left(\frac{-E_a}{RT}\right)\cdot f(\alpha) \quad (4)$$

where $f(\alpha)$ in Eqs. (1) and (4) can be expressed by different equations based on the reaction mechanism. The literature studies on the kinetic parameters of lignocellulosic biomass and/or its constituents from different models are presented in Table 5.

Other than TGA, Simultaneous Thermal Analysis (STA) is also one of the laboratory techniques to study the thermal degradation of lignocellulosic biomass [114]. During thermal treatment, STA can capture both mass changes and heating values at the same time. This approach has been validated for obtaining accurate heat reaction values [115]. Furthermore, the application of STA coupled with Fourier Transform Infrared spectroscopy (FT-IR) has been discovered and appeared to be an appealing method compared to the conventional thermogravimetric methods in the investigation of the thermal behavior of wood followed by oxidation reaction mechanisms [116]. This can be one of the advanced technologies to address the in-situ thermal behavior analysis on lignocellulosic biomass structure evolutions during the torrefaction process.

4.2. Scanning electron microscopy (SEM)

To obtain a deep insight into torrefaction towards lignocellulosic biomass, SEM is a crucial tool to study the morphology of biomass before and after torrefaction. Several magnification factors can be used to observe the microstructure images of the biomass surfaces. Fig. 4 shows an example of the SEM images of lignocellulosic biomass (bamboo) before and after torrefaction at temperatures of 200 °C (light torrefaction), 250 °C (mild torrefaction), and 300 °C (severe torrefaction) [82] under a magnification factor of 500.

For raw biomass, microfibers can be observed obviously on the surface. The effect of thermal pretreatment on biomass increased with torrefaction temperature. A study [102] observed that the particle surfaces consisted of tiny holes in bamboo and tubular structure in banyan under torrefaction temperature of 290 °C. In another study [117], the surfaces of torrefied coffee residues were smoother compared to the branched structure of raw material due to the degradation of hemicelluloses after torrefaction. Other than that, some microporous structures appeared on the surface of sawdust, indicating the damage of structure after torrefaction at 270 °C. The higher structural damage after torrefaction could be explained by the higher hemicellulose content in the biomass.

The study by Chen et al. [118] showed the effect of non-oxidative and oxidative torrefaction on the microstructures of fibrous and ligneous biomass. The non-oxidative and oxidative torrefaction showed

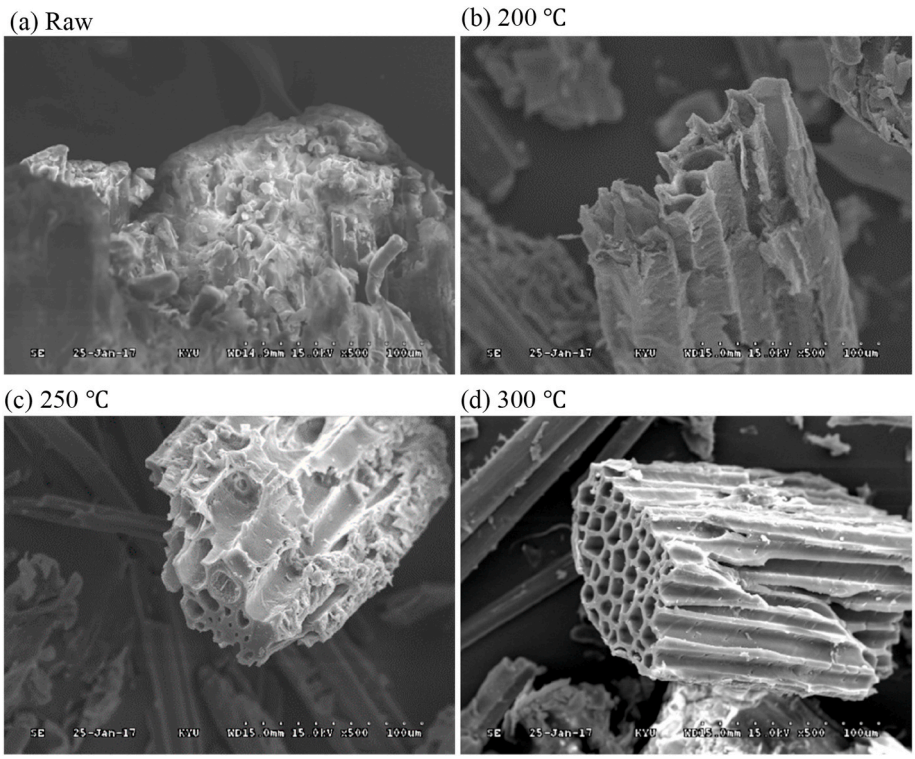

Fig. 4. Examples of SEM images of lignocellulosic biomass (bamboo) before and after torrefaction at temperatures of 200, 250, and 300 °C under magnification of 500 × .

a similar effect to the torrefied biomass structure. The raw oil palm fiber and coconut fiber showed an abundant amount of inclusions in the thick-walled fibers. The inclusions disappeared and the tubular structure was formed after torrefaction. This was due to the reduction of hemicellulose and lignin content in biomass. The alteration of microstructure showed a better grindability of biomass after torrefaction. Other than that, the study showed the SEM images of torrefied woodblock and compared them to raw biomass. The result showed that the torrefaction had a noticeable effect on the wood surface. When the exert temperature increased, the structure surface showed more damage and tubular structure. The result also showed filament features on torrefied wood (at particle size between 100 and 200 mesh) at the torrefaction temperature of 220 °C. However, the spherical shape of the particles could be observed when higher torrefaction temperatures (250 and 280 °C) were applied.

The study of the porous surface of raw empty fruit branches and palm mesocarp fiber showed that they were fibrous materials. The decomposition of the hemicelluloses was related to the internal structural changes of both materials after torrefaction. However, the depletion of lignin showed the least effect on the internal structure of the torrefied biomass. The study also showed the SEM images of raw willow and eucalyptus biomass with strong and bulky xylem tissues. The fibrous structure was damaged and the presence of more cracks and fissures in the particles occurred after torrefaction. This showed that torrefaction had a severe effect on the morphology and structural changes of lignocellulosic biomass based on SEM images.

Pores with a nanoscale size are not visible in SEM/FESEM imaging. Transmission electron microscopy (TEM) or high-resolution transmission electron microscopy (HR-TEM) can be the advanced method to confirm the presence of nanometer-size pores [119]. In electron microscopy, TEM is the most widely used method for the characterization of nanomaterials [120]. HR-TEM is an imaging mode of TEM imaging mode that enables direct imaging of the atomic structure of the material, and it can be considered as a useful technique for studying samples with atomic-scale characteristics [121]. In addition, there is a recent experimental method to carry out in-situ HR-TEM for the direct observation towards the microstructural evolution of the sample [122]. These advancements in the imaging technology can be applicable and helpful in future research on the characterization of lignocellulosic biomass-derived materials from torrefaction towards nanotechnology applications such as energy storage supercapacitors, etc.

4.3. Fourier transform infrared (FTIR) analysis

Fourier transform infrared spectroscopy is utilized to carry out FTIR analysis and to investigate the effect of torrefaction on the chemical structure of lignocellulosic biomass. The main band assignments of torrefied lignocellulosic biomass based on FTIR spectra are listed in Table 6, while the summary of typical FTIR absorption bands for lignocellulosic components is shown in Table 7.

Basically, there are noticeable effects of the FTIR spectra with torrefaction pretreatment. Most of the changes of FTIR spectra occur in the region of 1200–800 cm^{-1} due to the characteristics of polysaccharides, mainly hemicelluloses and cellulose [123–125]. The important functional groups to be studied are in the regions where most of the changes occur such as O–H, C═O, C═C, *C*–H, and *C*–O–C groups [126]. Hemicelluloses are known as the most reactive lignocellulosic components of biomass where notable decomposition reactions occur upon the torrefaction pretreatment [127,128]. The intensity of the peak decreases with the rising of torrefaction temperature. As the corresponding effect, this is due to the dehydration and decarboxylation reactions in the depletion of carbohydrates and the ester group removal through the deacetylation process of hemicelluloses [99]. The increase of the FTIR signal of aromatic and aliphatic groups suggests the increased degree of coalification upon torrefaction [129].

From a study [130] using the cotton stalk, there was a noticeable decrease in the FTIR spectra peak intensity of oxygen-containing functional groups, stemming from the depletion of organic substances, mainly hemicelluloses. The dehydroxylation and condensation reactions caused a decrease of the O–H peak at 3400-3200 cm^{-1}. The decreasing

Table 6
Main band assignments of torrefied lignocellulosic biomass based on FTIR spectra.

Functional group	Wavenumber (cm^{-1})	Explanation	Ref.
O–H (stretch)	3400–3200	O–H stretching to hydroxyl groups in phenolic and aliphatic structures	[32,124,126, 130,132, 234]
C–H (stretch)	3050–2800	i. *C*–H stretching of aromatic rings ii. Asymmetric vibrations of $–CH_2$ and symmetric vibrations of $–CH_2$	[124,131, 234–237]
C=O (stretch)	1600–1850; 1740-1710; 1516-1560	Carbonyl/carboxyl and ester groups in cellulose and hemicelluloses (including xylan)	[126, 129–132, 235–237]
C=C (stretch)	1640-1653; 1612-1450; 1596-1459	i. Stretching and skeletal vibrations of C=C aromatic ii. Aromatic skeletal vibrations of lignin	[60,124,126, 129,237]
C–H	1465–1426	i. Deformation of lignin and carbohydrates ii. The vibration of the aromatic rings in lignin and *C*–H bending in cellulose	[60,124,129, 237]
	1371–1382	Bending symmetric of –C–H (CH_3)	
	1376	Deformation of cellulose and hemicellulose	
	1320–1333	Vibration of cellulose	
C–O (stretch)	1333–1320	Vibration of syringyl derivatives	[32,60,99, 124,126,
	1269–1271	i. Attributed to a mode associated with the guaiacyl ring, *C*–O stretching in lignin and *C*–O linkage in guaiacyl aromatic methoxyl groups in softwood only ii. Aromatic *C*–O stretching of methoxyl and phenyl propane units	129, 236–238]
	1232	Attributed to a combination of deformation of the syringyl ring and a deformation of cellulose in softwood only	
	1246–1257	Syringyl ring in hardwoods only	
	1250-1220; 1160-1170	Antisymmetrical of *C*–O–C glycosidic bridge in cellulose and hemicelluloses	
	1157	*C*–O–C vibrations in cellulose and hemicellulose	
	1128–1134; 1147-1211	*C*–O stretching modes (*C*–O)	
	1006–1043	*C*–O stretching vibration and ether-type structures	
	899	Deformation in cellulose	
C–H (out-of-plane)	700–900	i. Three bands corresponding to out-of-plane deformation 1–4 adjacent *C*–H bonds in aromatic rings ii. Rocking of –(CH2)n- and bending (out-of-plane) of –HC=CH–(cis) iii. C–H due to aromatic structure in lignin	[28,31,129, 237,239]
O–H and *C*–C (out-of-plane)	640–701	Bending (out-of-plane) for O–H and *C*–C	[129]
C–C (stretch)	558	*C*–C stretching, aromatic rings	[240]

Table 7
Summary of typical FTIR absorption bands for lignocellulosic components.

Lignocellulosic component	Typical absorption bands/ Peaks (cm^{-1})	Ref.
Hemicellulose	1463, 1412, 1248, 1164, 1043, 987	[44,117]
Cellulose	1429, 1378, 1168, 1106, 1064, 1030, 897	[117, 241]
Lignin	1599, 1511, 1462, 1420	[45,117, 242]
Xylan	1725, 1601, 1460, 1407, 1382, 1312, 1250, 1212, 1163, 1110, 1079, 1038, 982, 895, 843, 780	[234]

of C=O peak at 1516-1560 cm^{-1} with increasing torrefaction temperature was caused by decarboxylation, and the breakage of glycosidic bonds and cyclic C=O along with the formation of oxygenated compounds and non-condensable gases [131]. The degradation of oxygen-containing organic groups showed effects on the simplified organic groups and thus had lower oxygen content. The study of Ibrahim and Darvell [126] showed that the functional groups that existed in torrefied biomass shifted towards lower wavenumbers and the alteration of peak intensity could be observed. The depletion of the O–H group in the torrefied biomass enhanced the hydrophobicity properties. Other than that, the depletion of hemicelluloses also resulted in the formation of more non-polar and unsaturated compounds in the torrefied samples. The torrefied sample would be more uniform with consistent quality based on the reduction of hemicelluloses and the enrichment of lignin. This could conclude that the torrefied sample could be qualified as a suitable feedstock for burning [132].

For the analysis of lignin fractions through FTIR, the typical bands at wavenumbers of 1600, 1510, and 1460 cm^{-1} representing the aromatic regions of lignin are decreased with increasing temperature, indicating the degradation of aromatic rings at higher temperatures [133,134]. Moreover, the ether and *C*–C linkages of lignin in torrefied biomass which consists of higher energy than other bonding show an increase of heating value and energy density after torrefaction [135]. Furthermore, a more detailed transformation of lignin structures in biomass after torrefaction still requires additional support from NMR spectral data that will be discussed further in Section 4.7. Besides, the study of Zheng et al. [27] on torrefied corncob showed the significant transformation of FTIR spectra occurred at the peak area of *C*–O–C asymmetrical vibration. The intensity of *C*–O–C vibration increased with increasing torrefaction temperature due to the cross-linking reaction on cellulose torrefaction. In the study of Nam and Capareda [135], there was a decrease of peak spectra at 897-898 cm^{-1} based on *C*–H deformation, as a consequence of the degradation of cellulose in the torrefied biomass [136].

According to the study of Sarvaramini et al. [137] on xylan torrefaction, the result showed that the degradation of xylan could not be carried out completely in mild conditions. This was owing to the decomposition that occurred at temperatures below 250 °C was subjected to the release of H_2O, CO, CO_2, methanol, aldehyde, and acetic products [138,139]. The carbonyl functional group (C=O) could act as a precursor for the study of the decomposition progress of xylan. However, when the torrefaction temperature was increased up to 280 °C, the breakage of glycosidic residues accompanying the release of furfurals, acids, water, and other gases took place [137]. This could be observed from the decrease of peak intensities at 950-1200 cm^{-1} (*C*–O bond stretching) and 3200-3600 cm^{-1} (O–H bond stretching) after torrefaction. In addition, the upward drifting of FTIR spectra towards the large wavenumber region indicated the formation of aromatic groups (at 1570 cm^{-1}) due to depletion of hydrogen and oxygen from xylan carbonization upon torrefaction. As a summary, the structural changes of lignocellulosic biomass from torrefaction are ranked from hemicelluloses to lignin, cellulose, and finally xylan [60,140].

Other than the conventional FTIR, advanced technologies such as

thermogravimetry coupled with Fourier transform infrared spectroscopy (TG-FTIR) and diffuse reflectance infrared Fourier transform spectroscopy (DRIFTS) have also been employed to make up for the deficiencies in current technologies on the structural analysis of lignocellulose biomass. The development of TG-FTIR is not only able to address the drawback in non-continuous analysis, the devolatilization and mass loss of biomass followed by the functional group identification of major volatiles species corresponding to a certain temperature range can also be monitored [141]. The behaviors of gas products and the emissions of SO_x, NO_x, and HCl pollutants from the torrefaction of cellulose, hemicelluloses, and lignin can be determined through TG-FTIR [142]. However, homodiatomic species such as H_2 cannot be measured, and there are difficulties in the identification of compounds with similar functional groups using TG-FTIR [143]. Therefore, TG-FTIR is preferable to be used on the final torrefaction products followed by speculation of the torrefaction mechanism based on the final product yield. To obtain more detailed and real-time information about the biomass structure changes throughout the torrefaction reaction process, in situ spectroscopy such as diffuse reflectance infrared Fourier transform spectroscopy (DRIFTS) is one of the excellent in-situ characterization methods [144,145]. The evolution in the functional groups can be monitored using DRIFTS to investigate the influence of structural differences in the lignocellulosic biomass during torrefaction. A recent study showed a new insight on the combination of in-situ DRIFTS with density functional theory (DFT) quantum chemical calculation in determining the effects of biomass component structures on pyrolysis [144]. This can be a new approach for future research in the monitoring of changes in lignocellulosic biomass structures while determining the possible torrefaction reaction paths of biomass with related information on the kinetic parameters [145].

4.4. X-ray diffraction (XRD)

4.4.1. Background and principle

X-ray diffraction (XRD) is an important method to study the sample crystallinity due to the diffraction peaks from cellulose crystals [146]. The principle of XRD analysis depends on the intensity of the spreading out and bending of light when it passes through a narrow aperture or across an edge which gives the structural information corresponding to the level of organization of the arrangement of a material's structure [147]. Due to constructive interference, an organized or ordered (crystalline) structure shows a sharp peak, attributing to the combined amplitude of superimposed waves. In contrast, a disorganized or disordered (amorphous) structure generates a smooth curve, resulting from destructive interference. The smooth curve generated by the random arrangement of atoms in space is a consequence of the cancellation of the intensities when the light scatters in all directions [147].

The crystallinity index (CrI) has been widely used to quantitatively describe the relative amount of crystalline and amorphous regions in the cellulose material [148]. It is defined as a ratio of the integrated area of the crystalline cellulose to the integrated total area of the peaks from both crystalline and amorphous cellulose [149]. Considering CrI calculation, there are three commonly used methods: (1) the Segal or peak height method [150]; (2) the peak deconvolution method; and (3) the amorphous subtraction method [151]. In the peak height method, CrI is expressed as shown in Eq. (5) [146,148]:

$$\mathrm{CrI}\ \ (\%) = \frac{I_{002} - I_{AM}}{I_{002}} \times 100 \tag{5}$$

where I_{002} is the height of the peak due to the diffraction plane of (002) at $2\theta = 23°$, and I_{AM} is the minimum height ($2\theta = 18°$) between peaks at (200) and (110). In fact, I_{002} corresponds to the maximum interference which represents crystalline and amorphous materials, while I_{AM} represents amorphous material. The second method involves the extraction of crystalline and amorphous contributions to the diffraction spectrum *via* a curve-fitting process, where the calculation is based on the intensity of the peaks at (110), (102), (200), or (004) for the cellulose and a single broad peak for amorphous parts [148,151]. The CrI calculation is done by dividing the peak areas of crystalline components by the total peak area [148,152]. The third method, which is also termed the Ruland-Vonk or amorphous contribution subtraction method [151], determines the crystallinity by subtracting the amorphous contribution from diffraction spectra using an amorphous standard. The CrI is defined and expressed as shown in equation (6):

$$\mathrm{CrI}\ \ (\%) = \frac{S_c}{S_t} \times 100 \tag{6}$$

where S_c is the area of the crystalline domain and S_t is the area of the total domain.

4.4.2. Studies of XRD on torrefaction

Several studies have been performed on the torrefaction of lignocellulosic biomass using XRD to analyze the structural transformation of the biomass from its raw state to its torrefied state. Three approaches have been utilized to present the pertinent data gathered from the analysis, either using a single approach or a combination of two approaches. The three approaches are: (1) comparison and discussion of the CrI values of raw and torrefied biomass; (2) identification and comparison of planes at evident peaks using peak deconvolution; and (3) tabulation and evaluation of other crystalline properties such as crystallite diameter and height [59,70,132,153–155].

Comparison and discussion of the crystallinity index values of the raw and torrefied biomass, namely, the first approach, have been reported in some literature studies. Neupane et al. [59] compared the CrI values of the raw loblolly pine and sweetgum to their torrefied counterparts at three different torrefaction temperatures (225, 250, 275 °C) and durations (15, 30, 45 min). Two peaks at the diffraction angles of 16° and 22° were seen in all the samples, except for the samples torrefied at the most severe conditions (275 °C & 45 min). The peak at $2\theta = 16°$ completely disappeared, implying the destruction of cellulose in the biomass.

Li et al. [156] carried out the torrefaction of bamboo in a carbon dioxide environment. They found that the CrI value decreased when the temperature increased, and no crystallinity was detected in the bamboo torrefied at 340 °C. It follows that the crystalline cellulose in the bamboo was completely destroyed. However, in another study by Li et al. [33], bamboo torrefaction in a nitrogen environment showed an increasing trend of the CrI value when the torrefaction severity increased, primarily due to the degradation of the amorphous components including hemicelluloses.

The study of Wannapeera and Worasuwannarak [155] showed torrefied leucaena in nitrogen at various combinations of torrefaction temperature and duration under desired solid yields (60%, 70%, and 80%) where the crystallinity of the torrefied leucaena was analyzed using an X-ray diffractometer. They observed that the peak intensities of the torrefied leucaenas at the angle range of $2\theta = 20–25°$ decreased with increasing torrefaction temperature along with a shorter duration. They mentioned that the decrease in the crystallinity of cellulose after the torrefaction might be attributed to the change in the intermolecular hydrogen bonding. Once the torrefaction was operated at 320 °C for 6 min with a solid yield of 60 wt%, no peak was observed, revealing that no crystalline cellulose remained.

Zhang et al. [140] studied biochars produced from the torrefaction of the cultivation residues of *Auricularia auricula-judae* where four different temperatures (200 °C, 240 °C, 280 °C, and 320 °C) and four different holding times (15 min, 30 min, 60 min, 120 min) were taken into account. Their results showed that, at the torrefaction temperatures of 200 and 240 °C for 60 min, the CrI values decreased slightly, from 40.06% to 38.59% and 38.89%, respectively. This indicated that hydrogen bonds were partly broken during the torrefaction processes. In contrast, for the

Table 8
Summary of CrI values of raw and torrefied biomass.

Feedstock	Torrefaction conditions	Remarks			Ref.
		22°	16°	CrI	
Loblolly pine and sweetgum	Temperature: 225, 250, 275 °C Duration: 15, 30, 45 min	The peak at all conditions was observed in both feedstock	No peak at highest temperature and duration	CrI of raw is 75.03% decreased to as low as 60.14% (275 °C-30 min) before cellulose disappeared at 275 °C-45 min	[59]
Bamboo	Temperature: 240, 260, 280, 300, 320, 340 °C Duration: 30 min *under CO_2 environment	No remarks	Complete destruction of crystallinity of cellulose at 340 °C	CrI of raw is 49.5%. Decreased from 46.1% to 19.1% (at 240–320 °C)	[154]
Bamboo	Temperature: 220, 240, 260, 280 °C Duration: 10, 30 and 60 min	No remarks	No remarks	CrI increased until 300 °C (from 47.97% to 55%)	[132]
Leucaena	Mass yield: 60% Prepared at: 280 °C - 105 min, 300 °C - 20 min, and 320 °C - 6 min	Peak evidently decreased with increasing torrefaction temperature; No peak at 320 °C-6 min	Peak diminished at 320 °C - 6 min	Not mentioned	[155]
Auricularia auricula-judae	Temperature: 200, 240, 280 and 320 °C Duration: 15, 30, 60 and 120 min	No remarks	No remarks	The lowest value for CrI (32.30%) was obtained at 320 °C-60 min	[70]
Pinus radiata	Torrefaction at (a) 250 °C for 45 min and at (b) 275 °C for 50 min	No remarks	No remarks	From 86.2%, the CrI values decreased to 85.0% and 69.8% respectively for a and b	[153]
Pine dust (Hammer and ball-milled)	Temperature: 230, 260 and 290 °C Duration: 30 and 60 min	No remarks	No remarks	The Lowest CrI values of HMP and BMP decreased from 31.10% to 24.95% and 11.5%–6.75%, respectively, at 290 °C-60 min	[157]

Table 9
The peak deconvolution of XRD curves at different torrefaction conditions.

Function	Conditions	Peaks	Remarks	Ref.
–	Temperature: 220 and 300 °C Duration: 30 min	$(1\bar{1}0)$ and (110)	Slight contraction at 220 and 300 °C compared to the control; indicates H-bonding change in the crystal	[158]
		(200)	Contracts by 0.1 Å at 220 and 300 °C; shows a slight decrease in distance between H-bond chains; increases hydrophobicity	
		(004)	No change	
Gaussian	Temperature: 230, 260, and 290 °C Duration: 30 and 60 min	(021)	The peak in raw HMP was not evident and appeared to be the left shoulder of (002); BMP showed a small sharp peak	[157]
		$(10\bar{1})$ and (101)	The two peaks are very close and formed a broad peak at around a diffraction angle of 16°	
		(002)	Disappeared in BMP curve due to covering of a broad amorphous cellulose peak	
Lorentzian	Temperature: 250 and 275 °C Duration: 45 and 50 min	(200)	A decrease indicates an increase in the spacing between the H-bonding cellulose crystal sheets	[153]
		$(1\bar{1}0)$ and (110)	Collapse indicates changes in H-bonding in the crystal sheet plane	

torrefaction temperature of 280 °C, the CrI value increased obviously when the duration increased until 60 min (CrI = 40.02%) but decreased at 120 min (CrI = 32.30%). The evident increase of crystallinity until 60 min was attributed to the degradation of hemicelluloses and the recrystallization of the amorphous region in cellulose. The lowest CrI value was obtained at 320 °C for 60 min, stemming from the dominant degradation of crystalline cellulose.

The study of Hill et al. [153] used the Lorentzian function to fit the major peaks, and the estimation on the proportion of surface to interior cellulose crystal chains was shown. The XRD analysis focused on the torrefaction of *Pinus radiata* at 250 °C for 45 min and 275 °C for 50 min. At a temperature of 250 °C for 45 min, the CrI value decreased from 86.2% to 85.0%, while at 275 °C for 50 min the CrI value decreased to 69.8%, indicating an evident cellulose chain degradation under these torrefaction conditions.

A summary of CrI values and remarks on two common diffraction angles (i.e., 16° and 22°) observed in cellulose is shown in Table 8. Generally, the CrI values of torrefied biomass at low temperatures and short durations are higher when compared to that of its parent biomass. This is attributed to the thermal degradation of hemicelluloses [70] and the recrystallization of amorphous components in cellulose [59,154]. When the torrefaction severity increases to a certain extent, the CrI value shows a decreasing trend with increasing temperature or duration. This reveals that the reduced crystallinities at high torrefaction severity are dominated by the degradation of crystalline cellulose.

For the second approach, three studies were involved [153,157,158]. Generally, the contractions and reductions are attributed to the increase in the spacing between the H-bonding which then results in the increased hydrophobicity of the material. A summary of the function used, torrefaction conditions, evaluated peaks, and specific remarks is shown in Table 9. As summarized in Table 9, Singh et al. [158] used the peak deconvolution method where the peaks $(1\bar{1}0)$, (110), (200), and (004) were involved. In their study, the radiata pine wood chips were subjected to a 30-min torrefaction at temperatures 220 and 300 °C, and the results showed that at peaks $(1\bar{1}0)$, (110) and (200), there was a small contraction in comparison to the raw biomass which indicated that the H-bonding in the crystal changed. The (004) peak did not pose any changes at both temperatures.

Gong et al. [157] investigated the ball-milled (BMP) and hammer-milled (HMP) pine dust for torrefaction. The CrI trends for both types followed the general trend of the CrI value, initially increasing and then showing a decrease. Comparing the two types, raw BMP had a lower CrI value (11.50%) than raw HMP (31.10%), hence the CrI values of torrefied BMP at all conditions were lower than CrI values of torrefied HMP. The lowest CrI values that the torrefied BMP and HMP obtained, which were 6.75% and 24.95% respectively, were the ones subjected at the highest torrefaction severity (at 290 °C for 60 min).

Table 10
Lattice parameters from X-ray diffraction analysis of raw and torrefied hardwood (RHW, THW), softwood (RSW, TSW), and sugar sorghum bagasse (RSB, TSB), respectively [159].

Samples	(002)	(110)	Interlayer spacing, (d_{002} (Å))	Crystalline height, (L_c (Å))	Crystalline size, (L_a (Å))	Number of crystallites in a stack, (N_{ave} (−))
RSW	25.8	40.2	4.01	28.4	100.4	8.08
TSW	25.7	40.3	4.02	27.5	71.8	7.84
RHW	25.9	40.7	3.99	29.3	91.4	8.33
THW	26.0	40.4	3.98	30.2	64.8	8.59
RSB	25.4	40.4	4.07	27.5	118.2	7.76
TSB	25.5	40.9	4.05	28.3	69.4	7.99

Lastly, among the nine studies of torrefaction that focused on XRD, only one made a further investigation of the crystallite height and crystalline size [159]. A summary of the lattice parameters from the XRD analysis of the raw and torrefied hardwood (RHW, THW), softwood (RSW, TSW), and sugar sorghum bagasse (RSB, TSB) is shown in Table 10. According to the tabulated data, the difference in the interlayer spacing and crystalline height of the raw and torrefied biomass for all samples was not evident. The change in the crystallite size might be dependent on the hemicellulose branching. The lower the order of branching, the smaller was the change (RSB > RSW > RHW).

The RHW and RSW showed an intense (002) peak at $2\theta = 26.1°$, while the peak for RSB shifted to 25.4° due to the stacking of graphitic basal planes. The values indicated that the orderliness of RHW and RSW was similar and that of RSB deviated considerably. After torrefaction, the (002) peak shifted to 25.7° and 24.6° for the woods and bagasse, respectively. A noticeable change in the diffractogram of THW and TSW was the peak at $2\theta = 31°$, which indicated the presence of calcium carbonate. At 51.2°, all the raw biomasses exhibited a sharp peak, attributing to the presence of the small amount of silicate compounds, which was intensified after torrefaction which indicating increased silica visibility. The initial increase of CrI value could be before being degraded at a higher temperature. The overall decrease in the crystallinity after torrefaction could be attributed to the change in the intermolecular hydrogen bonding [155].

Other than conventional XRD, there are also some recently developed technologies in the advancement of XRD such as Synchrotron X-ray diffraction (SXRD) and High-Temperature X-Ray Diffraction (HT-XRD). SXRD has been employed to study the microstructural changes in the sample where HT-XRD can characterize the evolution of the sample under steam and oxygen conditions with real-time tracking during the process [160,161]. Up to date, there is still limited study on the characterization of lignocellulosic biomass using these advanced XRD techniques. Further research can be carried out in the future using advanced XRD methods such as SXRD and HT-XRD for in-situ analysis to understand more detailed structural changes of lignocellulosic biomass during torrefaction.

4.5. Brunauer-Emmett-Teller (BET)

4.5.1. Background and principle

The Brunauer-Emmett-Teller (BET) theory plays a crucial role in measuring the specific surface area of a material. In fact, the theory is the most commonly used one for evaluating the specific surface area. The BET method is an extended Langmuir theory that focuses on the multilayer physical adsorption of gas molecules on the external and internal surfaces of material [162], in which the determination of the material's total specific surface area (m^2/g) depends on this phenomenon. The amount of the absorbed gas is dependent on its relative vapor pressure and the total external and internal surface of the material [163]. The data is treated using the BET adsorption isotherm equation as shown in Eq. (7):

$$\frac{X}{X_m} = \frac{C\left(p/p_o\right)}{\left(1 - p/p_o\right)\left(1 + (C-1)\,p/p_o\right)} \tag{7}$$

where X_m (g) is the mass of adsorbate forming a monolayer on a unit mass of adsorbent, X (g) the mass adsorbed at relative vapor pressure (p/p_o), p (Pa) the actual vapor pressure, p_o (Pa) the vapor pressure at saturation, and C (dimensionless) a constant which expresses the relative lifetime of molecules in the condensed state in each layer [163].

The method is established based on three hypotheses: (1) gas molecules physically adsorb on a solid in layers infinitely; (2) there is no interaction between each adsorption layer; and (3) the Langmuir theory can be applied to each theory [162].

4.5.2. Studies of BET method on torrefaction

A few torrefaction studies [126,159,164,165] mentioned the use of the BET method as part of the structural analysis. However, most studies concluded that there were no significant findings of the results. Among the four torrefaction studies that used the BET method, only one had an elaborated discussion about the results [159], two of which mentioned the BET values of torrefied biomass, but made no further discussion [126,164], and one declared its use on the raw and torrefied form of biomasses (pine and spruce) before subjected to explosion chamber [165].

Mafu et al. [159] investigated the torrefaction of softwood (SW), hardwood (HW), and sweet sorghum bagasse (SB) until the 30% mass loss was achieved at 260 °C. The mass loss was achieved at 110, 100, and 20 min for SW, HW, and SB, respectively. The raw SW (RSW) had the highest BET surface area which was 77 m^2/g, followed by RHW (62 m^2/g) then by RSB (15 m^2/g). After torrefaction, the BET surface areas of SW, HW, and SB were 68, 60, and 47 m^2/g, respectively. Only SB displayed an increase in BET surface area and no significant difference in the woody biomasses. The values in the BET surface areas of the torrefied biomass were attributed to the initial lignin content. They claimed that because lignin was softened and melt into the pores, the surface area decreased ascribing to the reduction of the accessible pore volume. Sweet sorghum bagasse had a very low lignin content, thus making it a viable candidate for having an increased BET surface area.

Ibrahim et al. [126] study showed the torrefied willow, eucalyptus, oak, and birch mixture (hardwood), spruce, pine, and larch (softwood) at three treatment conditions (270 °C for 30 min, 270 °C for 60 min, and 290 °C for 30 min), and reported that the surface areas of the torrefied materials fell within the range of 1.1–3.8 m^2/g. They mentioned that the BET surface area posed no significant pore development.

Arnsfeld et al. [164] torrefied two woody biomass samples (pine and beech wood) and three agricultural wastes products (palm kernel shells, pine kernel shells, and almond shells) and characterized them for gasification purposes. After torrefaction at different temperatures - pine wood and beech wood at 220, 250, and 300 °C, palm kernel at 250 and 300 °C, and pine kernel shells and almond shells at 300 °C – BET was conducted and the values for pinewood, beechwood, pine kernel shells, and almond shells were 1.63, 1.40, 1.37, and 1.70 m^2/g, respectively. No value was shown for the palm kernel shell and no remarks were made

concerning pore development.

The BET method is applied on the pore structure analysis of lignocellulosic biomass where the attribution of high non-structural carbohydrates content may be determined based on the pore volume [166]. Other than that, the amount of lignin content in biomass may also be part of the observation. The high lignin content results in a relatively small growth of surface area due to the reduction of accessible pore volume with the melting of lignin into pores after torrefaction [167]. The structural analysis of pore properties can also be used to assume the coalescence of biomass pores from the reduction of surface area after torrefaction [159,168]. In addition, the pore size is correlated with the torrefaction temperatures where the smaller pores with diameter <10 μm may coalesce into larger pores (>25 μm) at high temperature after torrefaction [164]. Further applications of the torrefied biomass can be determined based on the particular emphasis of the pore properties before and after torrefaction.

4.6. X-ray photoelectron spectroscopy (XPS)

4.6.1. Background and principle

X-ray photoelectron spectroscopy (XPS) is a quantitative technique that can determine the elemental composition, empirical formula, chemical state, and electronic state of material [169]. This technique measures the number of electrons emitted as a function of their kinetic energy when a material undergoes surface atom irradiation in an ultra-high vacuum (UHV) chamber with monoenergetic soft X-rays. The main principle of the analysis involves the photoelectric effect [170] where the incident X-ray may cause core electron emission of the molecule of the subjected material. When the threshold value is surpassed, however, only the electrons at the outermost layer of the material have the chance to escape. Therefore, the thickness considered for the analysis is only within 2–10 nm [170]. Considering lignocellulosic materials, two elements of carbon and oxygen are of particular interest and are detectable by XPS.

The binding energy of electrons in the 1s shell for C and O are 285 and 532 eV, respectively [170]. The C_{1s} signal detected by XPS is usually deconvoluted into four types of carbon atoms bonded to either other elements or functional groups; they are denoted as C_I, C_{II}, C_{III}, and C_{IV} [126,171]. The signal for C_I found at binding energy (BE) of 284.6 eV is attributed to carbon atoms bonded with carbon or hydrogen atoms only such as aromatic or aliphatic carbon (*C*–C, C═C, and *C*–H). The binding energy increases when the number of O atoms bonded to C increases. For this reason, the binding energy of C_I (284.6 eV) serves as the reference [171]. The signal for C_{II} is typically found at slightly higher BE ($\Delta BE = +1.5$ eV) compared to C_I and corresponds to a carbon atom bonded with one oxygen atom as well as ether or hydroxyl or phenyl groups (*C*–O-R). The signal for C_{III} ($\Delta BE = +2.9$ eV) corresponds to carbon atoms bonded to a carbonyl or two non-carbonyl oxygen atoms (C═O or O–*C*–O). C_{IV} ($\Delta BE = +4.2$ eV) is linked to carbon atoms bonded to a carbonyl and a non-carbonyl oxygen atom or carboxylic group or ester (-COO). In contrast, data for the BE of the O_{1s} signal are not completely clear, and the assignment of the oxygenated functional groups is still a matter of debate [126]. Nevertheless, the O_1 peak at BE of 531.4–532.3 eV has been tentatively assigned to carbonyl groups, while the signal for *C*–O-R groups is expected at 533.0–534.0 eV. The signal for moisture in wood is also expected to fall within the BE range of 533.0–533.5 eV for *C*–O-functionalities.

4.6.2. Studies of XPS on torrefaction

To date, there is limited literature on torrefaction studies using XPS as a tool to analyze the structures of lignocellulosic materials. Han et al. [171] investigated the torrefaction of *Eupatorium adenophorum* Spreng, a major invasive plant in southeast China, at 200, 225, 250, 275, 300, and 325 °C for 30 min. In their analysis, XPS survey scan spectra were

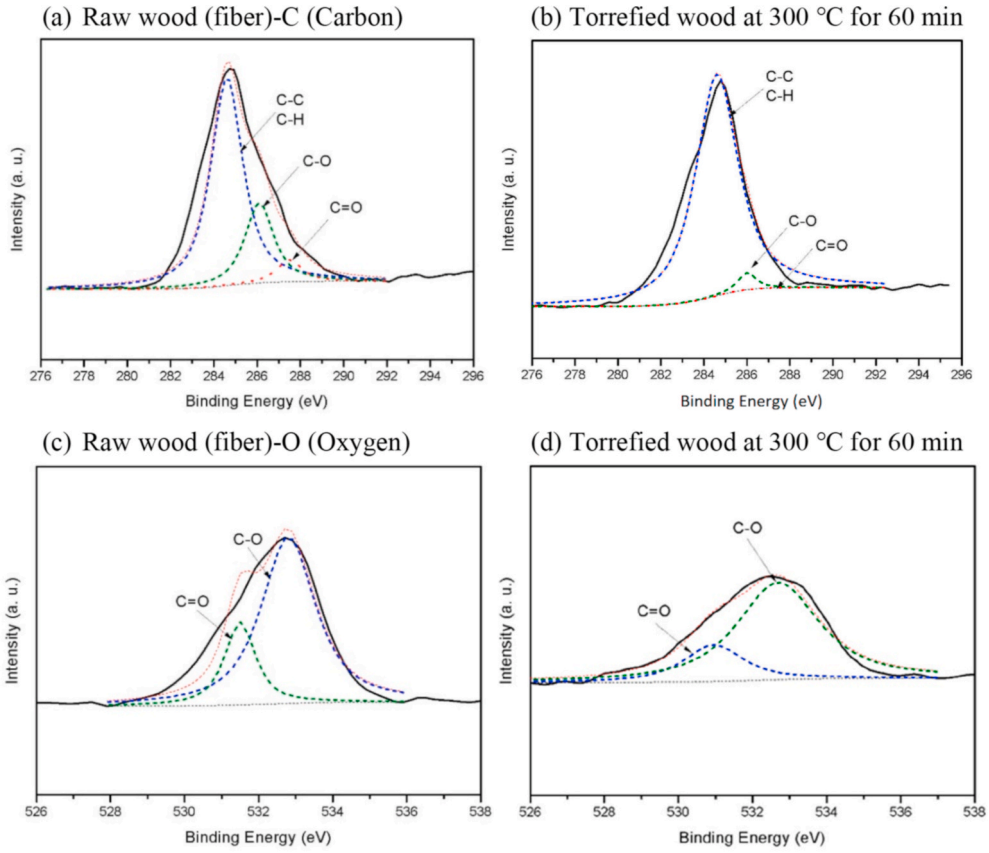

Fig. 5. X-ray Photoelectron Spectroscopy (XPS) result of carbon (a, b) and oxygen (c, d) on raw wood fiber and its torrefied sample, respectively.

recorded in pass energy of 100 eV and a binding energy range of 1200–0 eV by a step of 1 eV. High-resolution scanning of the C_{1s} region was performed in a step of 0.05 eV with a pass energy of 20 eV. For the raw biomass, the XPS analysis suggested that relative proportions (RPs) of the four types of C followed the order of $C_I > C_{II} > C_{III} > C_{IV}$. Once the torrefaction temperature increased, the RP of C_I increased from 52.23 to 73.39%, whereas C_{II} and C_{III} decreased from 39.40 to 19.72% and from 6.94 to 0.82%, respectively. As for C_{IV}, its RP values at each torrefaction temperature were close to each other. These data suggested the removal of O (reducing C_{II} and C_{III}) and enrichment of C (raising C_I) with increasing torrefaction temperature, so the torrefied biomass prepared at the higher temperature was more coal-like.

Ibrahim et al. [126] examined the XPS spectra of raw and torrefied eucalyptus. They observed that the deconvolution of the XPS spectra of the C_{1s} signal of the raw eucalyptus resulted in a large peak (at BE 284.6 eV) due to both C–C bonds and C–H (C_I type), which accounted for approximately 90% of the XPS signal. A smaller peak (10%) was found at BE of 287.5 eV, as the consequence of ether or hydroxyl (C_{II}) groups. The C_{1s} spectrum of the torrefied eucalyptus showed the disappearance of the ether or hydroxyl groups and a noticeable decrease of C_I, from 90% (the raw biomass) to 47%. The carbonyl groups (C_{III}) were also detected, which were absent from the raw sample. In the O_{1s} spectrum of the raw eucalyptus, a peak was observed at BE of 533.1 eV, resulting from ether groups (*C*–O–C), hydroxyl groups (*C*–OH), and possibly moisture. In a torrefied sample, the O_{1s} spectrum showed two peaks, with a large peak assigned to *C*–O–C or *C*–OH groups (533.3 eV) and a smaller peak at 531.5 eV possibly due to the formation of carbonyl groups. Their results of the XPS data were consistent with the observations from the FTIR spectroscopy, showing that torrefaction led to the loss of OH groups and the formation of C═O groups. On the account of dehydration reactions and cross-linking from torrefaction, the treated solids had a lower capability to hydrogen bond with water, and hence more hydrophobic.

The XPS results of carbon and oxygen on raw wood fiber and its torrefied sample are shown in Fig. 5. From Fig. 5b, the intensity of *C*–O and C═O bonds are reduced after torrefaction compared to raw material in Fig. 5a. This may be due to the breakage of bonding from the loss of H_2O, CO, and CO_2 in the sample. However, the intensities of *C*–C and *C*–H bonds increase, and this will lead to a decrease in conductivity in the torrefied sample after torrefaction. From Fig. 5d, there is a reduction in the percentages of C═O and *C*–O in the torrefied sample as compared to the raw sample in Fig. 5c. Although there is a significant reduction of C═O in torrefied samples, some C═O will be changed into the *C*–O bond after torrefaction.

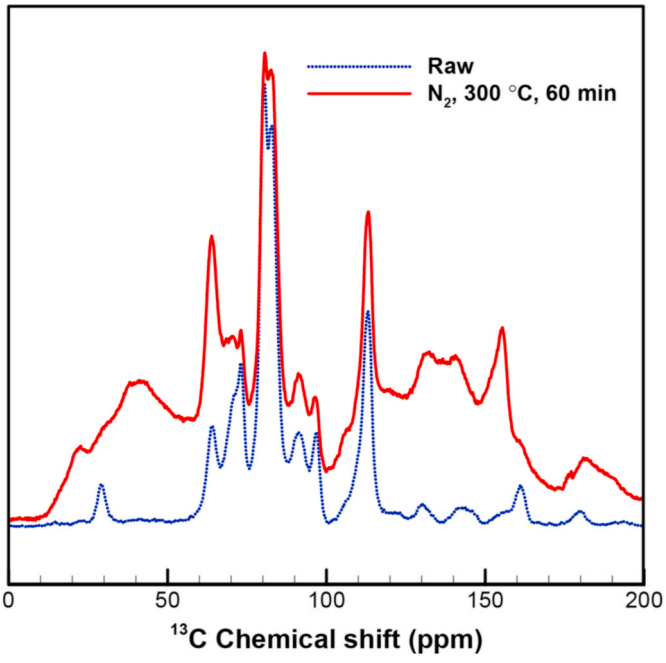

Fig. 6. ^{13}C high-resolution solid-state NMR spectra of raw and torrefied wood sawdust.

4.7. Nuclear magnetic resonance (NMR)

Nuclear magnetic resonance (NMR) has been commonly applied to study the chemical mechanisms that occurred during the torrefaction of lignocellulosic biomass. Since the analysis of solid char after torrefaction contributes to new insight on the mechanism of torrefaction reaction, the solid-state ^{13}C NMR analysis has been applied to study the structure of solid materials [172–174]. Due to the non-destructive method characteristics and no limitation on sample insolubility with detailed structural information, there is a wide application on char analysis using ^{13}C NMR [172,175]. In addition, the cross-polarization/magic angle spinning (CP/MAS) method is one of the most used NMR techniques in obtaining structural information of chars [172,175–178]. Analysis using CP/MAS provides chemical details of the samples at a short time with a good signal-to-noise ratio. However, the CP/MAS method cannot be considered as an accurate quantitative method due to its efficiency based on the magnetization transfer that is dependent on the environment of ^{13}C nuclei [68,179]. Fig. 6 shows the ^{13}C high-resolution solid-state NMR spectra of raw and torrefied wood sawdust. There are changes in the peaks of the chemical shift spectra before and after torrefaction. Each of the peaks corresponds to its relative main resonance assignment on the lignocellulosic component and chemical composition group based on the signal from ^{13}C NMR.

According to the study of Melkior et al. [174], the main conclusion that obtained from solid-state NMR was the extent of degradation that occurred at different lignocellulosic constituents. Hemicelluloses were the most degraded component at temperatures of 240–260 °C. The crystallinity of cellulose also increased when the temperature was above 200 °C, along with a slight effect on the lignin components. Even though the crosslinking reactions could be observed at temperatures above 260 °C, lignin components still appeared to be the most stable. The NMR analysis provides an insight into the de-acetylation of hemicelluloses, demethoxylation of lignin, and changes in the cellulose structure. As related, the study on the evaluation and comparison of the thermal reactivity of pine and beech woods under torrefaction using solid-state NMR also showed the main transformation mainly on the depletion of hemicelluloses. Other reactions such as demethoxylation, breaking of b-O-4 structures, and the formation of new chemical structures as related to the degradation of hemicelluloses was also investigated. The study on the torrefaction of Loblolly pine (*Pinus taeda*) also presented NMR spectra on the complete decomposition of hemicelluloses after the torrefaction at 250 °C for 4 h, with slight changes in the cellulose and lignin components.

The NMR tests in the study of pine, ash-wood, miscanthus, and wheat straw showed results that the chemical transformation of biomass functional groups was not directly correlated to the mass loss upon torrefaction [180]. High xylan content biomass materials such as ash-wood, miscanthus, and wheat straw had faster mass loss compared to pine with less xylan content. Lignin aided in protecting cellulose components and this caused a faster decomposition of non-woody biomass compared to woody biomass. From the study of Fu et al. [181], ^{13}C CP/MAS solid-state NMR spectroscopy was used to investigate the lignin content of kenaf biomass. The study suggested the application of solid-state NMR in lignin structural characterization of lignocellulosic biomass. With the understanding of solid-state NMR, the ^{13}C CP/MAS solid-state NMR method can be utilized in the application of papermaking, biomaterials analysis, tobacco analysis, biofuel, and bioethanol industries, in addition to research and industry related to plant and other biomass.

4.8. Advantages and limitations

In addition to the structural analysis, each of the methods possesses applications in the characterization of surface, structural, or molecular properties of lignocellulosic biomass. The analyses of SEM, FTIR, and BET discuss the surface characterization of the lignocellulosic sample before and after torrefaction while TGA, XRD, XPS, and NMR analyses provided information related to the structural and molecular properties changes of biomass throughout the torrefaction [182]. The characterization using SEM allows for the observation of the morphological changes of biomass before and after torrefaction through microscopic technique, where further qualitative and quantitative information on the composition, porosity, and finer structural details can be obtained [183]. However, the technique possesses a limitation on the resolution where minimum spot size can only be observed through scanning although better resolution can be achieved with modern instruments [184]. Further development on the quantification and measurement on an area basis for more particle and pore size distribution can be carried out to improve the analytical uncertainty of SEM technology [185]. FTIR is another potential microscopic analysis for biomass that can show details on the microscopic surface, it also shows details of the chemical and the molecular structures of the products before and after torrefaction [141]. To overcome the shortcomings in the application of conventional FTIR in structural analysis, coupling of FTIR with other techniques can be carried out to achieve the desirable analysis, TG-FTIR and DRIFTS are good examples. BET shows an important role in the characterization of biomass through measurement of specific surface area and is regarded as the most commonly used technique in the evaluation of pore properties in lignocellulosic biomass [186]. Nevertheless, BET theory possesses some limitations in certain materials analyses. With the overlook on the surface of the inhomogeneities, the analysis reflects that the characteristics of BET surface area differ from the real internal surface of the samples [187]. Other than that, a lot of manual preparation and analysis time are required for BET analysis. Although with some disadvantages in the technique, BET can be employed to study the surface area of nanoparticles but only towards dry samples or powders [188].

TGA is regarded as a useful characterization method in determining the thermal behavior and decomposition kinetics of lignocellulosic biomass [15,189]. The minimal sample preparation and simple sample handling with fast heating rate and precise control of the system conditions result in good resolution and high accuracy [190], TGA may be a time-saving and convenient characterization method in the study of biomass torrefaction. However, there are still some limitations of TGA since it is limited to samples that undergo weight loss, non-homogeneous samples cannot be analyzed [191]. In addition, the data interpretation is not straightforward and its sensitivity to heating rate and sample mass might also show effects in the shift in temperature. As opposite to TGA, XRD is a non-destructive technique in determining the chemical composition and structural arrangement of biomass samples, and it possesses a relatively straightforward data interpretation [185,192]. XRD can be a powerful and rapid characterization technique for the identification of unknown materials with minimal sample preparation and unambiguous mineral determination. However, XRD has a size limitation where large crystalline structures and homogeneous single-phase materials are preferable in the identification and analysis [193]. As related, XPS analysis acts as another non-destructive and efficient method in probing surface chemistry on the elemental composition, chemical state, etc, however, it also possesses a similar limitation on the sample size [194]. Other than that, the sample has to be compatible to be used in a high vacuum environment. The data interpretation of XPS can be straightforward with high content and chemical bonding information, but it has challenges in reproducibility as compared to other similar surface analysis techniques, and it is expensive [195]. NMR spectroscopy is also one of the powerful analytical methods for the identification of chemical composition in biomass [196]. The molecular and structure of the biomass samples can be elucidated through NMR analysis [197]. Other than FTIR, NMR can also be employed to determine the surface functional groups of torrefied biomass [182]. However, there are still some shortcomings with the low sensitivity and low natural abundance of the ^{13}C nuclei in the NMR application [196]. Further development towards different NMR approaches shall be carried out to improve ^{13}C NMR signals for better biomass analysis performance in the future.

5. Future challenges and perspectives

Torrefaction is one of the promising pretreatment technologies to produce solid or coal-like fuel in perspective for future bioenergy applications. The two different types of torrefaction, namely, dry torrefaction and wet torrefaction, have their own advantages and shortcomings in the applications of different sources of biomass. Dry torrefaction tends to produce a significant amount of ash content after the process which may lead to undesirable operation problems in industrial applications. However, wet torrefaction tends to have higher investment costs. Further research can be carried out to optimize both of the torrefaction processes in terms of energy-efficient and cost-effective for future large-scale commercial applications.

With the large availability of lignocellulosic biomass sources, the torrefaction process can be used to enhance biomass to produce more value-added products. According to the characterization analysis, torrefied lignocellulosic biomass shows an increase in higher heating value (HHV) which makes it a potential alternative of solid fuel to the current fossil fuels. On top of that, the imaging analysis of torrefied biomass also presents some structural changes with loopholes that make it suitable for application in adsorption studies. With the current characterization technique, the main chemical and structural transformation occurring under the influence of different torrefaction parameters can be easily predicted and evaluated on any other new raw lignocellulosic biomass. This will be one of the valuable techniques for the convenience of future research on the optimization of torrefaction conditions for commercial and sustainable applications.

Up to date, the torrefaction technology has been demonstrated on a pilot scale with the vision to upscale it for the application at a commercial scale with the production of around 50,000 tons/year and above [84]. Torrefaction technology is now still at the start-up phase in commercial development. Furthermore, the torrefaction demonstration plants also possess some technical problems that need to be sorted out that may lead to the delay in commercial operation progress. The torrefaction market is expected to keep growing and expand, however, there is limited available public information and knowledge related to the torrefaction technology and amounts of the torrefied biomass production. More research shall be carried out to achieve the vision for future large-scale commercial applications of torrefaction technology.

6. Conclusions

Torrefaction is an emerging pretreatment technology to enhance biomass properties toward green and sustainable energy systems. Lignocellulosic biomass is the most abundant and sustainable resource of biomass, the torrefied lignocellulosic biomass can produce solid fuel for bioenergy applications and other value-added products. Parameters such as temperature, residence time and heating rate play significant influencing roles in the torrefaction towards the final torrefied biomass properties where further optimization should be taken into account based on the desired application of the torrefied product. The application of produced biochars from torrefied lignocellulosic biomass is heavily dependent on their structural characteristics, therefore it is important to explore and understand the detailed structural change during the torrefaction process to optimize the application of the product. There are numerous structural analysis and characterization techniques available to examine the properties of torrefied biomass in

terms of thermal behavior, components, and morphological structure. With the current advanced characterization analysis technique, more valuable data can be easily obtained from the torrefaction conditions to optimize and enhance the current torrefaction process of lignocellulosic biomass. Furthermore, the development of advanced characterization also possesses contribution for in-situ analysis for the convenience in the understanding of biomass structural evolution throughout torrefaction. This makes torrefaction a promising potential technique for large-scale commercial implementation on bioenergy production in the near future.

Credit author statement

Hwai Chyuan Ong: Data collection, Methodology, Formal analysis, Validation, Visualization, Writing – review & editing. **Kai Ling Yu:** Data collection, Formal analysis, Investigation, Writing – review & editing. **Wei-Hsin Chen:** Conceptualization, Data collection, Formal analysis, Validation, Investigation, Visualization, Funding acquisition, Project administration, Resources, Writing – original draft. **Ma. Katreena Pillejera:** Data collection, Formal analysis, Methodology, Investigation, Writing – original draft. **Xiaotao Bi:** Investigation, Writing – review & editing. **Khanh-Quang Tran:** Investigation, Writing – review & editing. **Anelie Pétrissans:** Investigation, Writing – review & editing. **Mathieu Pétrissans:** Investigation, Writing – review & editing.

Declaration of competing interest

The authors declare that they have no known competing financial interests or personal relationships that could have appeared to influence the work reported in this paper.

Acknowledgments

The authors would like to acknowledge the financial support of the Ministry of Science and Technology, Taiwan, R.O.C., under the contracts MOST 109-2221-E-006-040-MY3, MOST 110-2622-E-006-001-CC1, and MOST 110-3116-F-006-003-. This research is also supported in part by the Higher Education Sprout Project, Ministry of Education to the Headquarters of University Advancement at National Cheng Kung University (NCKU). The authors gratefully acknowledge the use of EM000700, ESCA000200, and NMR000800 of 110-2731-M-006-001 belonging to the Core Facility Center of National Cheng Kung University.

References

[1] Nemitallah MA, Abdelhafez AA, Ali A, Mansir I, Habib MA. Frontiers in combustion techniques and burner designs for emissions control and CO2 capture: a review. Int J Energy Res 2019;43:7790–822.
[2] Chen W-H, Lu K-M, Tsai C-M. An experimental analysis on property and structure variations of agricultural wastes undergoing torrefaction. Appl Energy 2012;100:318–25.
[3] Sheldon RA. Green and sustainable manufacture of chemicals from biomass: state of the art. Green Chem 2014;16:950–63.
[4] Perlack RD WL, Turhollow AF, Graham RL, Stokes BJ, Erbach DC. Biomass as feedstock for a bioenergy and bioproducts industry: the technical feasibility of a billion-ton annual supply. TN: Oak Ridge National Lab2005.
[5] Nunes LJR, Causer TP, Ciolkosz D. Biomass for energy: a review on supply chain management models. Renew Sustain Energy Rev 2020;120:109658.
[6] Ubando AT, Felix CB, Chen W-H. Biorefineries in circular bioeconomy: a comprehensive review. Bioresour Technol 2020;299:122585.
[7] Zhou C-H, Xia X, Lin C-X, Tong D-S, Beltramini J. Catalytic conversion of lignocellulosic biomass to fine chemicals and fuels. Chem Soc Rev 2011;40:5588–617.
[8] Taarning E, Osmundsen CM, Yang X, Voss B, Andersen SI, Christensen CH. Zeolite-catalyzed biomass conversion to fuels and chemicals. Energy Environ Sci 2011;4:793–804.
[9] Mohan D, Pittman CU, Steele PH. Pyrolysis of wood/biomass for bio-oil: A critical review. Energy Fuel 2006;20:848–89.
[10] Sulaiman C, Abdul-Rahim AS, Ofozor CA. Does wood biomass energy use reduce CO2 emissions in European Union member countries? Evidence from 27 members. J Clean Prod 2020;253:119996.
[11] Ong HC, Chen W-H, Singh Y, Gan YY, Chen C-Y, Show PL. A state-of-the-art review on thermochemical conversion of biomass for biofuel production: a TG-FTIR approach. Energy Convers Manag 2020;209:112634.
[12] Goyal HB, Seal D, Saxena RC. Bio-fuels from thermochemical conversion of renewable resources: a review. Renew Sustain Energy Rev 2008;12:504–17.
[13] Chen W-H, Lin Y-Y, Liu H-C, Chen T-C, Hung C-H, Chen C-H, et al. A comprehensive analysis of food waste derived liquefaction bio-oil properties for industrial application. Appl Energy 2019;237:283–91.
[14] Xia C, Cai L, Zhang H, Zuo L, Shi SQ, Lam SS. A review on the modeling and validation of biomass pyrolysis with a focus on product yield and composition. Biofuel Res J 2021;8:1296–315.
[15] Chen W-H, Lin B-J, Lin Y-Y, Chu Y-S, Ubando AT, Show PL, et al. Progress in biomass torrefaction: principles, applications and challenges. Prog Energy Combust Sci 2021;82:100887.
[16] Arpia AA, Chen W-H, Lam SS, Rousset P, De Luna MDG. Sustainable biofuel and bioenergy production from biomass waste residues using microwave-assisted heating: a comprehensive review. Chem Eng J 2021:126233.
[17] Ong HC, Chen W-H, Farooq A, Gan YY, Lee KT, Ashokkumar V. Catalytic thermochemical conversion of biomass for biofuel production: a comprehensive review. Renew Sustain Energy Rev 2019;113:109266.
[18] SundarRajan P, Gopinath KP, Arun J, GracePavithra K, Adithya Joseph A, Manasa S. Insights into valuing the aqueous phase derived from hydrothermal liquefaction. Renew Sustain Energy Rev 2021;144:111019.
[19] Janajreh I, Adeyemi I, Raza SS, Ghenai C. A review of recent developments and future prospects in gasification systems and their modeling. Renew Sustain Energy Rev 2021;138:110505.
[20] Safar M, Lin B-J, Chen W-H, Langauer D, Chang J-S, Raclavska H, et al. Catalytic effects of potassium on biomass pyrolysis, combustion and torrefaction. Appl Energy 2019;235:346–55.
[21] Poudel J, Ohm T-I, Oh SC. A study on torrefaction of food waste. Fuel 2015;140:275–81.
[22] Prins MJ, Ptasinski KJ, Janssen FJJG. More efficient biomass gasification via torrefaction. Energy 2006;31:3458–70.
[23] Dehghani Madvar M, Aslani A, Ahmadi MH, Karbalaie Ghomi NS. Current status and future forecasting of biofuels technology development. Int J Energy Res 2019;43:1142–60.
[24] Lateef FA, Ogunsuyi HO. Jatropha curcas L. biomass transformation via torrefaction: surface chemical groups and morphological characterization. Curr Res Green Sustain Chem 2021:100142.
[25] Sun Y, Tong S, Li X, Wang F, Hu Z, Dacres OD, et al. Gas-pressurized torrefaction of biomass wastes: the optimization of pressurization condition and the pyrolysis of torrefied biomass. Bioresour Technol 2021;319:124216.
[26] Manouchehrinejad M, Bilek EMT, Mani S. Techno-economic analysis of integrated torrefaction and pelletization systems to produce torrefied wood pellets. Renew Energy 2021;178:483–93.
[27] Zheng A, Zhao Z, Chang S, Huang Z, Wang X, He F, et al. Effect of torrefaction on structure and fast pyrolysis behavior of corncobs. Bioresour Technol 2013;128:370–7.
[28] Toscano G, Pizzi A, Foppa Pedretti E, Rossini G, Ciceri G, Martignon G, et al. Torrefaction of tomato industry residues. Fuel 2015;143:89–97.
[29] Chen W-H, Wang C-W, Ong HC, Show PL, Hsieh T-H. Torrefaction, pyrolysis and two-stage thermodegradation of hemicellulose, cellulose and lignin. Fuel 2019;258:116168.
[30] Poudel J, Oh S. Effect of torrefaction on the properties of corn stalk to enhance solid fuel qualities. Energies 2014;7:5586.
[31] Park S-W, Jang C-H, Baek K-R, Yang J-K. Torrefaction and low-temperature carbonization of woody biomass: evaluation of fuel characteristics of the products. Energy 2012;45:676–85.
[32] Pushkin SA, Kozlova LV, Makarov AA, Grachev AN, Gorshkova TA. Cell wall components in torrefied softwood and hardwood samples. J Anal Appl Pyrol 2015;116:102–13.
[33] Li M-F, Chen C-Z, Li X, Shen Y, Bian J, Sun R-C. Torrefaction of bamboo under nitrogen atmosphere: influence of temperature and time on the structure and properties of the solid product. Fuel 2015;161:193–6.
[34] Bentsen NS, Felby C, Thorsen BJ. Agricultural residue production and potentials for energy and materials services. Prog Energy Combust Sci 2014;40:59–73.
[35] Chen W-H, Du S-W, Tsai C-H, Wang Z-Y. Torrefied biomasses in a drop tube furnace to evaluate their utility in blast furnaces. Bioresour Technol 2012;111:433–8.
[36] Scott MJ, Jones MN. The biodegradation of surfactants in the environment. Biochim Biophys Acta Biomembr 2000;1508:235–51.
[37] Popp J, Lakner Z, Harangi-Rákos M, Fári M. The effect of bioenergy expansion: food, energy, and environment. Renew Sustain Energy Rev 2014;32:559–78.
[38] Tursi A. A review on biomass: importance, chemistry, classification, and conversion. Biofuel Res J 2019;6:962–79.
[39] Wang SLZ. Pyrolysis of biomass. 2016.
[40] Vorwerk S, Somerville S, Somerville C. The role of plant cell wall polysaccharide composition in disease resistance. Trends Plant Sci 2004;9:203–9.
[41] Heredia AJA, Guillén R. Composition of plant cell walls, vol. 200. European Food Research and Technology; 1995. p. 24–31.
[42] Adila Maisyarah Mansor, Lim Jeng Shiun, Farid Nasir Ani, Hashim Haslenda, Ho WS. Characteristics of cellulose, hemicellulose and lignin of MD2 pineapple biomass. Chem Eng Tran 2019;72.
[43] Scheller HV, Ulvskov P. Hemicelluloses. Annu Rev Plant Biol 2010;61:263–89.
[44] Chaikumpollert O, Methacanon P, Suchiva K. Structural elucidation of hemicelluloses from Vetiver grass. Carbohydr Polym 2004;57:191–6.

[45] Sun JX, Sun XF, Sun RC, Fowler P, Baird MS. Inhomogeneities in the chemical structure of sugarcane bagasse lignin. J Agric Food Chem 2003;51:6719–25.
[46] Katahira R, Elder TJ, Beckham GT. Chapter 1. A brief introduction to lignin structure. Lignin Valorization 2018:1–20.
[47] Stoilova IKA, Stanchev V. Properties of crude laccase from Trametes versicolor produced by solid-substrate fermentation. Adv Biosci Biotechnol 2010;1:2368.
[48] Alonso DM, Bond JQ, Dumesic JA. Catalytic conversion of biomass to biofuels. Green Chem 2010;12:1493–513.
[49] Chen W-H, Kuo P-C. Torrefaction and co-torrefaction characterization of hemicellulose, cellulose and lignin as well as torrefaction of some basic constituents in biomass. Energy 2011;36:803–11.
[50] J BM. Thermochem Proc Biomass 2011.
[51] Sankaran R, Cruz RAP, Pakalapati H, Show PL, Ling TC, Chen W-H, et al. Recent advances in the pretreatment of microalgal and lignocellulosic biomass: a comprehensive review. Bioresour Technol 2020;298:122476.
[52] Anca-Couce A. Reaction mechanisms and multi-scale modelling of lignocellulosic biomass pyrolysis. Prog Energy Combust Sci 2016;53:41–79.
[53] Dhyani V, Bhaskar T. A comprehensive review on the pyrolysis of lignocellulosic biomass. Renew Energy 2017.
[54] Hu Y, Wang S, Wang Q, He Z, Abomohra AE-F, Cao B. Influence of torrefaction pretreatment on the pyrolysis characteristics of seaweed biomass. Cellulose 2019;26:8475–87.
[55] Bach Q-V, Ø Skreiberg. Upgrading biomass fuels via wet torrefaction: a review and comparison with dry torrefaction. Renew Sustain Energy Rev 2016;54:665–77.
[56] Acharya B, Sule I, Dutta A. A review on advances of torrefaction technologies for biomass processing. Biomass Conv Bioref 2012;2:349–69.
[57] Uemura Y, Matsumoto R, Saadon S, Matsumura Y. A study on torrefaction of Laminaria japonica. Fuel Process Technol 2015;138:133–8.
[58] IEA. Task 40, Possible effects of torrefaction on biomass trade. 2015.
[59] Neupane S, Adhikari S, Wang Z, Ragauskas AJ, Pu Y. Effect of torrefaction on biomass structure and hydrocarbon production from fast pyrolysis. Green Chem 2015;17:2406–17.
[60] Zheng A, Jiang L, Zhao Z, Huang Z, Zhao K, Wei G, et al. Impact of torrefaction on the chemical structure and catalytic fast pyrolysis behavior of hemicellulose, lignin, and cellulose. Energy Fuel 2015;29:8027–34.
[61] Chen D, Gao A, Cen K, Zhang J, Cao X, Ma Z. Investigation of biomass torrefaction based on three major components: hemicellulose, cellulose, and lignin. Energy Convers Manag 2018;169:228–37.
[62] Chen W-H, Lin B-J, Huang M-Y, Chang J-S. Thermochemical conversion of microalgal biomass into biofuels: a review. Bioresour Technol 2015;184:314–27.
[63] Chen D, Zhou J, Zhang Q, Zhu X, Lu Q. Torrefaction of rice husk using TG-FTIR and its effect on the fuel characteristics, carbon, and energy yields, vol. 2014; 2014. p. 9.
[64] Roberts KG, Gloy BA, Joseph S, Scott NR, Lehmann J. Life cycle assessment of biochar systems: estimating the energetic, economic, and climate change potential. Environ Sci Technol 2010;44:827–33.
[65] Mašek O, Budarin V, Gronnow M, Crombie K, Brownsort P, Fitzpatrick E, et al. Microwave and slow pyrolysis biochar—comparison of physical and functional properties. J Anal Appl Pyrol 2013;100:41–8.
[66] Prins MJ, Ptasinski KJ, Janssen FJJG. Torrefaction of wood: Part 2. Analysis of products. J Anal Appl Pyrol 2006;77:35–40.
[67] Medic D, Darr M, Shah A, Potter B, Zimmerman J. Effects of torrefaction process parameters on biomass feedstock upgrading. Fuel 2012;91:147–54.
[68] Ben H, Ragauskas AJ. Torrefaction of loblolly pine. Green Chem 2012;14:72–6.
[69] Gucho E, Shahzad K, Bramer E, Akhtar N, Brem G. Experimental study on dry torrefaction of beech wood and miscanthus. Energies 2015;8:3903.
[70] Mei Y, Che Q, Yang Q, Draper C, Yang H, Zhang S, et al. Torrefaction of different parts from a corn stalk and its effect on the characterization of products. Ind Crop Prod 2016;92:26–33.
[71] Almeida G, Brito JO, Perré P. Alterations in energy properties of eucalyptus wood and bark subjected to torrefaction: the potential of mass loss as a synthetic indicator. Bioresour Technol 2010;101:9778–84.
[72] Tumuluru JS, Sokhansanj S, Wright CT, Boardman RD, Hess JR. Review on biomass torrefaction process and product properties and design of moving bed torrefaction system model development. America. 2011.
[73] Nunes LJR, Matias JCO, Catalão JPS. A review on torrefied biomass pellets as a sustainable alternative to coal in power generation. Renew Sustain Energy Rev 2014;40:153–60.
[74] Abdulyekeen KA, Umar AA, Patah MFA, Daud WMAW. Torrefaction of biomass: production of enhanced solid biofuel from municipal solid waste and other types of biomass. Renew Sustain Energy Rev 2021;150:111436.
[75] Yu KL, Lau BF, Show PL, Ong HC, Ling TC, Chen W-H, et al. Recent developments on algal biochar production and characterization. Bioresour Technol 2017;246:2–11.
[76] Zhang Y, Geng P, Liu R. Synergistic combination of biomass torrefaction and co-gasification: reactivity studies. Bioresour Technol 2017;245:225–33.
[77] Barskov S, Zappi M, Buchireddy P, Dufreche S, Guillory J, Gang D, et al. Torrefaction of biomass: a review of production methods for biocoal from cultured and waste lignocellulosic feedstocks. Renew Energy 2019;142:624–42.
[78] Peng J, Bi H, Sokhansanj S, Lim J. A study of particle size effect on biomass torrefaction and densification. Energy Fuel 2012;26:3826–39.
[79] Tsamba AJ, Yang W, Blasiak W. Pyrolysis characteristics and global kinetics of coconut and cashew nut shells. Fuel Process Technol 2006;87:523–30.
[80] Yang H, Yan R, Chen H, Zheng C, Lee DH, Liang DT. In-depth investigation of biomass pyrolysis based on three major Components: hemicellulose, cellulose and lignin. Energy Fuel 2006;20:388–93.
[81] Ru B, Wang S, Dai G, Zhang L. Effect of torrefaction on biomass physicochemical characteristics and the resulting pyrolysis behavior. Energy Fuel 2015;29:5865–74.
[82] Chen W-H, Kuo P-C. A study on torrefaction of various biomass materials and its impact on lignocellulosic structure simulated by a thermogravimetry. Energy 2010;35:2580–6.
[83] Kamdem DPPA, Jermannaud A. Durability of heat-treated wood. Eur J Wood Wood Prod 2002;60:1–6.
[84] Eseyin AE, Steele PH, Pittman Jr CU. Current trends in the production and applications of torrefied wood/biomass-A review. BioResources 2015;10:8812–58.
[85] Thrän D, Witt J, Schaubach K, Kiel J, Carbo M, Maier J, et al. Moving torrefaction towards market introduction – technical improvements and economic-environmental assessment along the overall torrefaction supply chain through the SECTOR project. Biomass Bioenergy 2016;89:184–200.
[86] Walton R, Bommel B. A complete and comprehensive overview of torrefaction technologies. E-EnergyMarket; 2011.
[87] Agbor E, Zhang X, Kumar A. A review of biomass co-firing in North America. Renew Sustain Energy Rev 2014;40:930–43.
[88] Bergman P, Boersma A, Zwart R, Kiel J. Torrefaction for biomass Co-firing in existing coal-fired power stations. Energy research Centre of the Netherlands; 2005.
[89] Chen W-H, Lin B-J, Colin B, Chang J-S, Pétrissans A, Bi X, et al. Hygroscopic transformation of woody biomass torrefaction for carbon storage. Appl Energy 2018;231:768–76.
[90] Wang L, Riva L, Ø Skreiberg, Khalil R, Bartocci P, Yang Q, et al. Effect of torrefaction on properties of pellets produced from woody biomass. Energy Fuel 2020;34:15343–54.
[91] Chen W-H, Huang M-Y, Chang J-S, Chen C-Y. Torrefaction operation and optimization of microalga residue for energy densification and utilization. Appl Energy 2015;154:622–30.
[92] Zaini IN, Novianti S, Nurdiawati A, Irhamna AR, Aziz M, Yoshikawa K. Investigation of the physical characteristics of washed hydrochar pellets made from empty fruit bunch. Fuel Process Technol 2017;160:109–20.
[93] Saddawi A, Jones JM, Williams A, Le Coeur C. Commodity fuels from biomass through pretreatment and torrefaction: effects of mineral content on torrefied fuel characteristics and quality. Energy Fuel 2012;26:6466–74.
[94] Demirbas A. Potential applications of renewable energy sources, biomass combustion problems in boiler power systems and combustion related environmental issues. Prog Energy Combust Sci 2005;31:171–92.
[95] Wannapeera J, Worasuwannarak N. Upgrading of woody biomass by torrefaction under pressure. J Anal Appl Pyrol 2012;96:173–80.
[96] Yan B, Jiao L, Li J, Zhu X, Ahmed S, Chen G. Investigation on microwave torrefaction: parametric influence, TG-MS-FTIR analysis, and gasification performance. Energy 2021;220:119794.
[97] Mamvura TA, Danha G. Biomass torrefaction as an emerging technology to aid in energy production. Heliyon 2020;6:e03531.
[98] Chaiwong K, Kiatsiriroat T, Vorayos N, Thararax C. Biochar production from freshwater algae by slow pyrolysis. Maejo Int J Sci Technol 2012;6.
[99] Park J, Meng J, Lim KH, Rojas OJ, Park S. Transformation of lignocellulosic biomass during torrefaction. J Anal Appl Pyrol 2013;100:199–206.
[100] Chen W-H, Kuo P-C. Isothermal torrefaction kinetics of hemicellulose, cellulose, lignin and xylan using thermogravimetric analysis. Energy 2011;36:6451–60.
[101] Wang Z, Lim CJ, Grace JR, Li H, Parise MR. Effects of temperature and particle size on biomass torrefaction in a slot-rectangular spouted bed reactor. Bioresour Technol 2017;244:281–8.
[102] Chen W-H, Cheng W-Y, Lu K-M, Huang Y-P. An evaluation on improvement of pulverized biomass property for solid fuel through torrefaction. Appl Energy 2011;88:3636–44.
[103] Bridgeman TG, Jones JM, Shield I, Williams PT. Torrefaction of reed canary grass, wheat straw and willow to enhance solid fuel qualities and combustion properties. Fuel 2008;87:844–56.
[104] Bousquet J. THERMAL data for natural and synthetic fuels by siddhartha gaur (VSLR sciences -Dallas, TX)and Thomas B.REED. (Colorado School of Mines-Golden, CO)Marcel DEKKER; 1988. p. 258. Price 167, 71 euros. The Canadian Journal of Chemical Engineering. 2005;83:389-.
[105] Golova OP. Chemical effects of heat on cellulose. Russ Chem Rev 1975;44:687.
[106] Patai S, Halpern Y. Pyrolytic reaction of carbohydrates. Part IX the effect of additives on the thermal behavior of cellulose samples of different crystallinity. Isr J Chem 1970;8:655–62.
[107] Mansaray KG, Ghaly AE. Thermal degradation of rice husks in nitrogen atmosphere. Bioresour Technol 1998;65:13–20.
[108] Antal MJ. Biomass pyrolysis: a review of the literature Part 1—carbohydrate pyrolysis. In: Böer KW, Duffie JA, editors. Advances in solar energy: an annual review of research and development, 1 · 1982. Boston, MA: Springer New York; 1985. p. 61–111.
[109] Chen W-H, Peng J, Bi XT. A state-of-the-art review of biomass torrefaction, densification and applications. Renew Sustain Energy Rev 2015;44:847–66.
[110] Ninan K. Kinetics of solid state thermal decomposition reactions. J Therm Anal 1989;35:1267–78.
[111] White JE, Catallo WJ, Legendre BL. Biomass pyrolysis kinetics: a comparative critical review with relevant agricultural residue case studies. J Anal Appl Pyrol 2011;91:1–33.

[112] Bach Q-V, Chen W-H, Chu Y-S, Ø Skreiberg. Predictions of biochar yield and elemental composition during torrefaction of forest residues. Bioresour Technol 2016;215:239–46.
[113] Bach Q-V, Chen W-H. Pyrolysis characteristics and kinetics of microalgae via thermogravimetric analysis (TGA): a state-of-the-art review. Bioresour Technol 2017;246:88–100.
[114] Arvelakis S, Jensen PA, Dam-Johansen K. Simultaneous thermal analysis (STA) on ash from high-alkali biomass. Energy Fuel 2004;18:1066–76.
[115] Rath J, Wolfinger MG, Steiner G, Krammer G, Barontini F, Cozzani V. Heat of wood pyrolysis. Fuel 2003;82:81–91.
[116] Candelier K, Dibdiakova J, Volle G, Rousset P. Study on chemical oxidation of heat treated lignocellulosic biomass under oxygen exposure by STA-DSC-FTIR analysis. Thermochim Acta 2016;644:33–42.
[117] Chen W-H, Lu K-M, Tsai C-M. An experimental analysis on property and structure variations of agricultural wastes undergoing torrefaction. Appl Energy 2012;100:318–25.
[118] Chen W-H, Tsai M-H, Hung C-I. Characterization of transient CO_2transport in two convecting aerosol droplets in Tandem. Aerosol Air Q Res 2014;14:207–19.
[119] Venkateshaiah A, Padil VVT, Nagalakshmaiah M, Waclawek S, Černík M, Varma RS. Microscopic techniques for the analysis of micro and nanostructures of biopolymers and their derivatives. Polymers 2020;12.
[120] Kumar PS, Pavithra KG, Naushad M. Characterization techniques for nanomaterials. Nanomaterials for solar cell applications. Elsevier; 2019. p. 97–124.
[121] Shanmuga Priya M, Divya P, Rajalakshmi R. A review status on characterization and electrochemical behaviour of biomass derived carbon materials for energy storage supercapacitors. Sustain Chem Pharm 2020;16:100243.
[122] Sharma S, Shyam Kumar CN, Korvink JG, Kübel C. Evolution of glassy carbon microstructure: in situ transmission electron microscopy of the pyrolysis process. Sci Rep 2018;8:16282.
[123] Haykiri-Acma H, Yaman S. Thermogravimetric investigation on the thermal reactivity of biomass during slow pyrolysis. Int J Green Energy 2009;6:333–42.
[124] Bilgic E, Yaman S, Haykiri-Acma H, Kucukbayrak S. Limits of variations on the structure and the fuel characteristics of sunflower seed shell through torrefaction. Fuel Process Technol 2016;144:197–202.
[125] Rani M, Rudhziah S, Ahmad A, Mohamed N. Biopolymer electrolyte based on derivatives of cellulose from kenaf bast fiber. Polymers 2014;6:2371.
[126] Ibrahim RHH, Darvell LI, Jones JM, Williams A. Physicochemical characterisation of torrefied biomass. J Anal Appl Pyrol 2013;103:21–30.
[127] Di Blasi C. Modeling chemical and physical processes of wood and biomass pyrolysis. Prog Energy Combust Sci 2008;34:47–90.
[128] Rousset P, Aguiar C, Labbé N, Commandré J-M. Enhancing the combustible properties of bamboo by torrefaction. Bioresour Technol 2011;102:8225–31.
[129] Benavente V, Fullana A. Torrefac Olive Mill Waste Biomass Bioenergy 2015;73:186–94.
[130] Chen D, Zheng Z, Fu K, Zeng Z, Wang J, Lu M. Torrefaction of biomass stalk and its effect on the yield and quality of pyrolysis products. Fuel 2015;159:27–32.
[131] Chen D, Zhou J, Zhang Q, Zhu X, Lu Q. Torrefaction of rice husk using TG-FTIR and its effect on the fuel characteristics, carbon, and energy yields. BioResources 2014;9.
[132] Zia F, Zia KM, Zuber M, Kamal S, Aslam N. Starch based polyurethanes: a critical review updating recent literature. Carbohydr Polym 2015;134:784–98.
[133] Wen J-L, Sun S-L, Yuan T-Q, Xu F, Sun R-C. Understanding the chemical and structural transformations of lignin macromolecule during torrefaction. Appl Energy 2014;121:1–9.
[134] Wen JL, Sun SL, Xue BL, Sun RC. Quantitative structural characterization of the lignins from the stem and pith of bamboo (Phyllostachys pubescens). Holzforschung 2013;67:613–27.
[135] Nam H, Capareda S. Experimental investigation of torrefaction of two agricultural wastes of different composition using RSM (response surface methodology). Energy 2015;91:507–16.
[136] Chang S, Zhao Z, Zheng A, He F, Huang Z, Li H. Characterization of products from torrefaction of sprucewood and bagasse in an auger reactor. Energy Fuel 2012;26:7009–17.
[137] Sarvaramini A, Assima GP, Larachi F. Dry torrefaction of biomass – torrefied products and torrefaction kinetics using the distributed activation energy model. Chem Eng J 2013;229:498–507.
[138] Shen DK, Gu S, Bridgwater AV. Study on the pyrolytic behaviour of xylan-based hemicellulose using TG–FTIR and Py–GC–FTIR. J Anal Appl Pyrol 2010;87:199–206.
[139] Lv P, Almeida G, Perré P. TGA-FTIR analysis of torrefaction of lignocellulosic components (cellulose, xylan, lignin) in isothermal conditions over a wide range of time durations. 2015.
[140] Zhang Y, Yao A, Song K. Torrefaction of cultivation residue of Auricularia auricula-judae to obtain biochar with enhanced fuel properties. Bioresour Technol 2016;206:211–6.
[141] Wang S, Dai G, Yang H, Luo Z. Lignocellulosic biomass pyrolysis mechanism: a state-of-the-art review. Prog Energy Combust Sci 2017;62:33–86.
[142] Ren Q, Zhao C. NO x and N2O precursors from biomass pyrolysis: role of cellulose, hemicellulose and lignin. Environ Sci Technol 2013;47:8955–61.
[143] Biagini E, Barontini F, Tognotti L. Devolatilization of biomass fuels and biomass components studied by TG/FTIR technique. Ind Eng Chem Res 2006;45:4486–93.
[144] Wang G, Dai G, Ding S, Wu J, Wang S. A new insight into pyrolysis mechanism of three typical actual biomass: the influence of structural differences on pyrolysis process. J Anal Appl Pyrol 2021;156:105184.
[145] Elmay Y, Brech YL, Delmotte L, Dufour A, Brosse N, Gadiou R. Characterization of Miscanthus pyrolysis by DRIFTs, UV Raman spectroscopy and mass spectrometry. J Anal Appl Pyrol 2015;113:402–11.
[146] Thygesen A, Oddershede J, Lilholt H, Thomsen AB, Ståhl K. On the determination of crystallinity and cellulose content in plant fibres. Cellulose 2005;12:563.
[147] Cullity BD. Elements of X-ray diffraction. Massachusetts: Addison-Wesley publishing company, inc.; 1956.
[148] Park S, Baker JO, Himmel ME, Parilla PA, Johnson DK. Cellulose crystallinity index: measurement techniques and their impact on interpreting cellulase performance. Biotechnol Biofuels 2010;3:10.
[149] Rodriguez Alonso E, Dupont C, Heux L, Da Silva Perez D, Commandre J-M, Gourdon C. Study of solid chemical evolution in torrefaction of different biomasses through solid-state 13C cross-polarization/magic angle spinning NMR (nuclear magnetic resonance) and TGA (thermogravimetric analysis). Energy 2016;97:381–90.
[150] Segal L, Creely JJ, Martin AE, Conrad CM. An empirical method for estimating the degree of crystallinity of native cellulose using the x-ray diffractometer. Textil Res J 1962;29.
[151] Karimi K, Taherzadeh MJ. A critical review of analytical methods in pretreatment of lignocelluloses: composition, imaging, and crystallinity. Bioresour Technol 2016;200:1008–18.
[152] Wang Z, McDonald AG, Westerhof RJM, Kersten SRA, Cuba-Torres CM, Ha S, et al. Effect of cellulose crystallinity on the formation of a liquid intermediate and on product distribution during pyrolysis. J Anal Appl Pyrol 2013;100:56–66.
[153] Hill SJ, Grigsby WJ, Hall PW. Chemical and cellulose crystallite changes in Pinus radiata during torrefaction. Biomass Bioenergy 2013;56:92–8.
[154] Chen W-H, Liu S-H, Juang T-T, Tsai C-M, Zhuang Y-Q. Characterization of solid and liquid products from bamboo torrefaction. Appl Energy 2015;160:829–35.
[155] Wannapeera J, Worasuwannarak N. Examinations of chemical properties and pyrolysis behaviors of torrefied woody biomass prepared at the same torrefaction mass yields. J Anal Appl Pyrol 2015;115:279–87.
[156] Li M-F, Li X, Bian J, Xu J-K, Yang S, Sun R-C. Influence of temperature on bamboo torrefaction under carbon dioxide atmosphere. Ind Crop Prod 2015;76:149–57.
[157] Gong C, Huang J, Feng C, Wang G, Tabil L, Wang D. Effects and mechanism of ball milling on torrefaction of pine sawdust. Bioresour Technol 2016;214:242–7.
[158] Singh T, Singh AP, Hussain I, Hall P. Chemical characterisation and durability assessment of torrefied radiata pine (Pinus radiata) wood chips. Int Biodeterior Biodegrad 2013;85:347–53.
[159] Mafu LD, Neomagus HWJP, Everson RC, Carrier M, Strydom CA, Bunt JR. Structural and chemical modifications of typical South African biomasses during torrefaction. Bioresour Technol 2016;202:192–7.
[160] Zino R, Chosson R, Ollivier M, Serris E. Breakaway characterization of Zircaloy-4 oxidized in steam and in oxygen at high temperatures using HT-XRD analysis. Corrosion Sci 2020;176:109028.
[161] Dutta A, Dey S, Gayathri N, Mukherjee P, Roy TK, Sagdeo A, et al. Microstructural evolution of proton irradiated Fe-2.25Cr–1Mo characterized using synchrotron XRD (SXRD). Radiat Phys Chem 2021;184:109459.
[162] Brunauer S, Emmett PH, Teller E. Adsorption of gases in multimolecular layers. J Am Chem Soc 1938;60:309–19.
[163] Fagerlund G. Determination of specific surface by the BET method. Matériaux et Construction. 1973;6:239–45.
[164] Arnsfeld S, Senk D, Gudenau HW. The qualification of torrefied wooden biomass and agricultural wastes products for gasification processes. J Anal Appl Pyrol 2014;107:133–41.
[165] Medina CH, Phylaktou HN, Andrews GE, Gibbs BM. Explosion characteristics of pulverised torrefied and raw Norway spruce (Picea abies) and Southern pine (Pinus palustris) in comparison to bituminous coal. Biomass Bioenergy 2015;79:116–27.
[166] Downie A, Crosky A, Munroe P. Physical properties of biochar. Biochar for environmental management: Routledge; 2012. p. 45–64.
[167] Xue G, Kwapinska M, Horvat A, Kwapinski W, Rabou L, Dooley S, et al. Gasification of torrefied Miscanthus× giganteus in an air-blown bubbling fluidized bed gasifier. Bioresour Technol 2014;159:397–403.
[168] Guerrero M, Ruiz MP, Millera Á, Alzueta MU, Bilbao R. Characterization of biomass chars formed under different devolatilization conditions: differences between rice husk and eucalyptus. Energy Fuel 2008;22:1275–84.
[169] Watts JF, Wolstenholme J. An introduction to surface analysis by XPS and AES. England: John Wiley and Sons Ltd; 2003.
[170] Pickering KL. Properties and performance of natural-fibre composites. New Zealand: Woodhead publishing limited and Maney publishing limited; 2008.
[171] Han Z, Zeng X, Yao C, Xu G. Oxygen migration in torrefaction of eupatorium adenophorum Spreng. And its improvement on fuel properties. Energy Fuel 2015;29:7275–83.
[172] Le Brech Y, Raya J, Delmotte L, Brosse N, Gadiou R, Dufour A. Characterization of biomass char formation investigated by advanced solid state NMR. Carbon 2016;108:165–77.
[173] Freitas JCC, Bonagamba TJ, Emmerich FG. Investigation of biomass- and polymer-based carbon materials using 13C high-resolution solid-state NMR. Carbon 2001;39:535–45.
[174] Melkior T, Jacob S, Gerbaud G, Hediger S, Le Pape L, Bonnefois L, et al. NMR analysis of the transformation of wood constituents by torrefaction. Fuel 2012;92:271–80.
[175] Mao J, Hu W, Ding G, Schmidt-Rohr K, Davies G, Ghabbour E, et al. Suitability of different 13C solid-state NMR techniques in the characterization of humic acids. Int J Environ Anal Chem 2002;82:183–96.

[176] Cao X, Pignatello JJ, Li Y, Lattao C, Chappell MA, Chen N, et al. Characterization of wood chars produced at different temperatures using advanced solid-state 13C NMR spectroscopic techniques. Energy Fuel 2012;26:5983–91.
[177] Freitas JCC, Bonagamba TJ, Emmerich FG. 13C high-resolution solid-state NMR study of peat carbonization. Energy Fuel 1999;13:53–9.
[178] Zhang X, Golding J, Burgar I. Thermal decomposition chemistry of starch studied by 13C high-resolution solid-state NMR spectroscopy. Polymer 2002;43:5791–6.
[179] Sharma RK, Wooten JB, Baliga VL, Lin X, Geoffrey Chan W, Hajaligol MR. Characterization of chars from pyrolysis of lignin. Fuel 2004;83:1469–82.
[180] Alonso ER, Dupont C, Heux L, Perez DDS, Commandre J-M, Gourdon C. Study of solid chemical evolution in torrefaction of different biomasses through solid-state 13C cross-polarization/magic angle spinning NMR (nuclear magnetic resonance) and TGA (thermogravimetric analysis). Energy 2016;97:381–90.
[181] Fu L, McCallum SA, Miao J, Hart C, Tudryn GJ, Zhang F, et al. Rapid and accurate determination of the lignin content of lignocellulosic biomass by solid-state NMR. Fuel 2015;141:39–45.
[182] Yaashikaa PR, Kumar PS, Varjani S, Saravanan A. A critical review on the biochar production techniques, characterization, stability and applications for circular bioeconomy. Biotechnol Rep 2020;28:e00570.
[183] Sørensen HS, Rosenberg P, Petersen HI, Sørensen LH. Char porosity characterisation by scanning electron microscopy and image analysis. Fuel 2000; 79:1379–88.
[184] Chaffey N, Hayat MA. Principles and techniques of electron microscopy: biological applications. fourth ed. Cambridge: Cambridge University Press; 2000. p. 543. £65 (hardback). Annals of Botany. 2001;87:546-548.
[185] Bahng M-K, Mukarakate C, Robichaud DJ, Nimlos MR. Current technologies for analysis of biomass thermochemical processing: a review. Anal Chim Acta 2009; 651:117–38.
[186] Meng X, Ragauskas AJ. Recent advances in understanding the role of cellulose accessibility in enzymatic hydrolysis of lignocellulosic substrates. Curr Opin Biotechnol 2014;27:150–8.
[187] McMillan W, Teller E. The assumptions of the BET theory. J Phys Chem 1951;55: 17–20.
[188] Raja PMV, Barron AR. BET surface area analysis of nanoparticles. 2021.
[189] Chen R, Kirsh Y. The analysis of thermally stimulated processes. Elsevier; 2013.
[190] Decker J, Walker AH, Bosnick K, Clifford C, Dai L, Fagan J, et al. Sample preparation protocols for realization of reproducible characterization of single-wall carbon nanotubes. Metrologia 2009;46:682.
[191] Moseson DE, Jordan MA, Shah DD, Corum ID, Alvarenga Jr BR, Taylor LS. Application and limitations of thermogravimetric analysis to delineate the hot melt extrusion chemical stability processing window. Int J Pharm 2020;590: 119916.
[192] Warren B. X-ray diffraction. New York: Dover publications; 1990. p. 253.
[193] Bunaciu AA, UdriŞTioiu EG, Aboul-Enein HY. X-ray diffraction: instrumentation and applications. Crit Rev Anal Chem 2015;45:289–99.
[194] Oswald S. X-Ray photoelectron spectroscopy in analysis of surfaces. Encyclopedia of Analytical Chemistry: Applications, Theory and Instrumentation 2006.
[195] Inari GN, Pétrissans M, Dumarcay S, Lambert J, Ehrhardt J, Šernek M, et al. Limitation of XPS for analysis of wood species containing high amounts of lipophilic extractives. Wood Sci Technol 2011;45:369–82.
[196] Emwas A-HM. The strengths and weaknesses of NMR spectroscopy and mass spectrometry with particular focus on metabolomics research. Metabonomics: Springer; 2015. p. 161–93.
[197] Abriata LA, Zaballa M-E, Berry RE, Yang F, Zhang H, Walker FA, et al. Electron spin density on the axial His ligand of high-spin and low-spin Nitrophorin 2 probed by heteronuclear NMR spectroscopy. Inorg Chem 2013;52:1285–95.
[198] Dai L, Wang Y, Liu Y, Ruan R, Yu Z, Jiang L. Comparative study on characteristics of the bio-oil from microwave-assisted pyrolysis of lignocellulose and triacylglycerol. Sci Total Environ 2019;659:95–100.
[199] Jiang L-q, Wu Y-x, Wang X-b, Zheng A-q, Zhao Z-l, Li H-b, et al. Crude glycerol pretreatment for selective saccharification of lignocellulose via fast pyrolysis and enzyme hydrolysis. Energy Convers Manag 2019;199:111894.
[200] Peterson CA, Lindstrom J, Polin J, Cady SD, Brown RC. Oxidation of phenolic compounds during autothermal pyrolysis of lignocellulose. J Anal Appl Pyrol 2020:104853.
[201] Cao X, Zhong L, Peng X, Sun S, Li S, Liu S, et al. Comparative study of the pyrolysis of lignocellulose and its major components: characterization and overall distribution of their biochars and volatiles. Bioresour Technol 2014;155:21–7.
[202] Zabeti M, Baltrusaitis J, Seshan K. Chemical routes to hydrocarbons from pyrolysis of lignocellulose using Cs promoted amorphous silica alumina catalyst. Catal Today 2016;269:156–65.
[203] Nsaful F, Collard F-X, Carrier M, Görgens JF, Knoetze JH. Lignocellulose pyrolysis with condensable volatiles quantification by thermogravimetric analysis—thermal desorption/gas chromatography–mass spectrometry method. J Anal Appl Pyrol 2015;116:86–95.
[204] Wang Z, Lin W, Song W, Wu X. Pyrolysis of the lignocellulose fermentation residue by fixed-bed micro reactor. Energy 2012;43:301–5.
[205] Ratnasari DK, Yang W, Jönsson PG. Two-stage ex-situ catalytic pyrolysis of lignocellulose for the production of gasoline-range chemicals. J Anal Appl Pyrol 2018;134:454–64.
[206] Zabeti M, Nguyen TS, Lefferts L, Heeres HJ, Seshan K. In situ catalytic pyrolysis of lignocellulose using alkali-modified amorphous silica alumina. Bioresour Technol 2012;118:374–81.
[207] Mašek O, Budarin V, Gronnow M, Crombie K, Brownsort P, Fitzpatrick E, et al. Microwave and slow pyrolysis biochar—comparison of physical and functional properties. J Anal Appl Pyrol 2013;100:41–8.
[208] Yan W, Acharjee TC, Coronella CJ, Vásquez VR. Thermal pretreatment of lignocellulosic biomass. Environ Prog Sustain Energy 2009;28:435–40.
[209] Wang Z, Lim CJ, Grace JR. A comprehensive study of sawdust torrefaction in a dual-compartment slot-rectangular spouted bed reactor. Energy 2019;189: 116306.
[210] Zhang Y, Song K. Thermal and chemical characteristics of torrefied biomass derived from a generated volatile atmosphere. Energy 2018;165:235–45.
[211] Bridgeman T, Jones J, Shield I, Williams P. Torrefaction of reed canary grass, wheat straw and willow to enhance solid fuel qualities and combustion properties. Fuel 2008;87:844–56.
[212] Chen D, Chen F, Cen K, Cao X, Zhang J, Zhou J. Upgrading rice husk via oxidative torrefaction: characterization of solid, liquid, gaseous products and a comparison with non-oxidative torrefaction. Fuel 2020;275:117936.
[213] Babinszki B, Jakab E, Sebestyén Z, Blazsó M, Berényi B, Kumar J, et al. Comparison of hydrothermal carbonization and torrefaction of azolla biomass: analysis of the solid products. J Anal Appl Pyrol 2020;149:104844.
[214] Manatura K. Inert torrefaction of sugarcane bagasse to improve its fuel properties. Case Stud Therm Eng 2020;19:100623.
[215] Zheng N-Y, Lee M, Lin Y-L. Co-processing textile sludge and lignocellulose biowaste for biofuel production through microwave-assisted wet torrefaction. J Clean Prod 2020:122200.
[216] Hu J, Song Y, Liu J, Evrendilek F, Buyukada M, Yan Y, et al. Combustions of torrefaction-pretreated bamboo forest residues: physicochemical properties, evolved gases, and kinetic mechanisms. Bioresour Technol 2020;304:122960.
[217] Tian X, Dai L, Wang Y, Zeng Z, Zhang S, Jiang L, et al. Influence of torrefaction pretreatment on corncobs: a study on fundamental characteristics, thermal behavior, and kinetic. Bioresour Technol 2020;297:122490.
[218] Singh RK, Chakraborty JP, Sarkar A. Optimizing the torrefaction of pigeon pea stalk (cajanus cajan) using response surface methodology (RSM) and characterization of solid, liquid and gaseous products. Renew Energy 2020;155: 677–90.
[219] Wang N, Zhan H, Zhuang X, Xu B, Yin X, Wang X, et al. Torrefaction of waste wood-based panels: more understanding from the combination of upgrading and denitrogenation properties. Fuel Process Technol 2020;206:106462.
[220] Brachi P, Chirone R, Miccio M, Ruoppolo G. Fluidized bed torrefaction of biomass pellets: a comparison between oxidative and inert atmosphere. Powder Technol 2019;357:97–107.
[221] Zhang Y, Chen F, Chen D, Cen K, Zhang J, Cao X. Upgrading of biomass pellets by torrefaction and its influence on the hydrophobicity, mechanical property, and fuel quality. Biomass Conversion and Biorefinery; 2020.
[222] Tumuluru JS, Sokhansanj S, Wright CT, Hess JR, Boardman RD. A review on biomass torrefaction process and product properties. In: Symposium on thermochemical conversion. Stillwater, OK: Oklahoma State University; 2011.
[223] Chen W-H, Lin B-J, Colin B, Petrissans A, Petrissans M. A study of hygroscopic property of biomass pretreated by torrefaction. In: The 15th international symposium on district heating and cooling; 2018.
[224] Jaya Shankar Tumuluru SS, Richard Hess J, Wright Christopher T, Boardman Richard D. A review on biomass torrefaction process and product properties for energy applications. 2011.
[225] Niu Y, Lv Y, Lei Y, Liu S, Liang Y, Wang D, et al. Biomass torrefaction: properties, applications, challenges, and economy. Renew Sustain Energy Rev 2019;115.
[226] Zhang C, Ho S-H, Chen W-H, Xie Y, Liu Z, Chang J-S. Torrefaction performance and energy usage of biomass wastes and their correlations with torrefaction severity index. Appl Energy 2018;220:598–604.
[227] Ren S, Lei H, Wang L, Bu Q, Chen S, Wu J. Thermal behaviour and kinetic study for woody biomass torrefaction and torrefied biomass pyrolysis by TGA. Biosyst Eng 2013;116:420–6.
[228] Oluoti K, Doddapaneni TRKC, Richards T. Investigating the kinetics and biofuel properties of Alstonia congensis and Ceiba pentandra via torrefaction. Energy 2018;150:134–41.
[229] Toptas A, Yildirim Y, Duman G, Yanik J. Combustion behavior of different kinds of torrefied biomass and their blends with lignite. Bioresour Technol 2015;177: 328–36.
[230] Brachi P, Miccio F, Miccio M, Ruoppolo G. Isoconversional kinetic analysis of olive pomace decomposition under torrefaction operating conditions. Fuel Process Technol 2015;130:147–54.
[231] Bach Q-V, Tran K-Q, Ø Skreiberg. Comparative study on the thermal degradation of dry- and wet-torrefied woods. Appl Energy 2017;185:1051–8.
[232] Pasangulapati V, Kumar A, Jones CL, Huhnke RL. Characterization of switchgrass, cellulose, hemicellulose and lignin for thermochemical conversions. J Biobased Mater Bioenergy 2012;6:249–58.
[233] Yang H, Yan R, Chin T, Liang DT, Chen H, Zheng C. Thermogravimetric Analysis–Fourier transform infrared analysis of palm oil waste pyrolysis. Energy Fuel 2004;18:1814–21.
[234] Lv P, Almeida G, Perré P. TGA-FTIR analysis of torrefaction of lignocellulosic components (cellulose, xylan, lignin) in isothermal conditions over a wide range of time durations. BioResources 2015;10.
[235] Chen W-H, Lin M-R, Leu T-S, Du S-W. An evaluation of hydrogen production from the perspective of using blast furnace gas and coke oven gas as feedstocks. Int J Hydrogen Energy 2011;36:11727–37.
[236] Pala M, Kantarli IC, Buyukisik HB, Yanik J. Hydrothermal carbonization and torrefaction of grape pomace: a comparative evaluation. Bioresour Technol 2014; 161:255–62.
[237] Pohlmann JG, Osório E, Vilela ACF, Diez MA, Borrego AG. Integrating physicochemical information to follow the transformations of biomass upon torrefaction and low-temperature carbonization. Fuel 2014;131:17–27.

[238] Pandey KK. A study of chemical structure of soft and hardwood and wood polymers by FTIR spectroscopy. J Appl Polym Sci 1999;71:1969–75.
[239] Via BK, Adhikari S, Taylor S. Modeling for proximate analysis and heating value of torrefied biomass with vibration spectroscopy. Bioresour Technol 2013;133:1–8.
[240] Wilk M, Magdziarz A, Kalemba I. Characterisation of renewable fuels' torrefaction process with different instrumental techniques. Energy 2015;87:259–69.
[241] Liu CF, Xu F, Sun JX, Ren JL, Curling S, Sun RC, et al. Physicochemical characterization of cellulose from perennial ryegrass leaves (Lolium perenne). Carbohydr Res 2006;341:2677–87.
[242] Chen WH, Tu YJ, Sheen HK. Disruption of sugarcane bagasse lignocellulosic structure by means of dilute sulfuric acid pretreatment with microwave-assisted heating. Appl Energy 2011;88:2726–34.